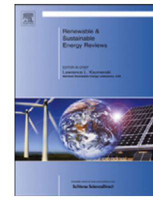
Renewable and Sustainable Energy Reviews 16 (2012) 5207–5224

Contents lists available at SciVerse ScienceDirect

Renewable and Sustainable Energy Reviews

journal homepage: www.elsevier.com/locate/rser



Thermochemical energy storage and conversion: A-state-of-the-art review of the experimental research under practical conditions

Jaume Cot-Gores, Albert Castell, Luisa F. Cabeza*

GREA Innovació Concurrent, Edifici CREA, Universitat de Lleida, Pere de Cabrera s/n, 25001 Lleida, Spain

A R T I C L E I N F O

Article history:
Received 17 January 2012
Accepted 1 April 2012
Available online 28 June 2012

Keywords:
Thermal storage
Chemical heat pump
Solid–gas
Refrigeration
Chemical heat transformer
Thermochemical energy storage

A B S T R A C T

Thermal energy storage and conversion aims to improve the high inefficiency of the industrial processes and renewable energy systems (supply versus demand). Chemical sorption processes and chemical reactions based on solid–gas systems are a promising way to store and convert thermal energy for heating or cooling applications and, thereby to increase the efficiency of the processes and to reduce the greenhouse effect. Although more efforts are required to bring this technology to the market, some important breakthrough have been made regarding to system efficiency. Over the last two decades, the experimental research in this field has increased largely to validate these advances under practical conditions. Therefore, this paper gives a state-of-art review of performances obtained under practical conditions by the different prototypes built over the last two decades. In addition, the main advantages and disadvantages of solid–gas chemical sorption processes and chemical reactions are summarized.

Contents

1. Introduction

The increased demand for energy, the rise in the price of fuel associated with the depletion of fossil fuels, and the growth of CO_2 emissions all require the development of more energy-efficient processes and a shift from non-renewable energy sources to renewable energy sources. In this sense, thermal energy storage and conversion (TESC) can increase the thermal energy efficiency of a process by reusing the waste heat from industrial

Abbreviations: AC, activated carbon; CFC, chlorofluorocarbons; CHP, chemical heat pump; CHPD, chemical heat pump dryer; EG, expanded graphite; G, reactive gas; HCFC, hydrochlorofluorocarbons; HT, high temperature; LT, low temperature; S, reactive salt; S′, produced compound; TESC, thermal energy storage and conversion

* Corresponding author. Tel.: +34 973003576; fax: +34 973003575.
E-mail address: lcabeza@diei.udl.cat (L.F. Cabeza).

1364-0321/$ - see front matter © 2012 Elsevier Ltd. All rights reserved.
http://dx.doi.org/10.1016/j.rser.2012.04.007

Nomenclature

COA	coefficient of amplification
COP	coefficient of performance
COPA	combined coefficient of performance and amplification
ΔH	Enthalpy change (J mol^{-1})
ΔS	Entropy change (J mol^{-1} K^{-1})
P	pressure (Pa)
R	gas constant (J mol^{-1} K^{-1})
SCP	specific cooling power (W kg^{-1})
SHP	specific heating power (W kg^{-1})
T	temperature (°C)

Subscripts

c	cooling
d	driving
eq	equilibrium
h	high
l	low
m	medium

processes, solar energy or other sources. Furthermore, considering that in 2004 the heating and cooling demands of the industrial, commercial and domestic sector accounted for between 40–50 % of the total global 320 EJ (7,639 Mtoe) final energy demand [1], TESC could contribute to substantial energy savings and a reduction in CO_2 emissions [2].

Heat is the form of energy most widely used in industry and power plants for driving the processes or producing electricity, either through steam or in fired furnaces. As a consequence of the work produced, most of this heat is degraded to a lower level and is released to the environment through cooling water, cooling towers, flue gases or other means (Fig. 1). This waste heat is left unused due to its relatively low grade. TESC not only allows the waste heat to be re-used, it also allows the heat to be upgraded by means of a chemical heat pump. Furthermore, when the thermal demand is located at a distance from the supply, this heat could be transported [4].

Even in diesel or gasoline engines, TESC can be used to recover the waste heat lost through the radiator or the exhaust. For instance, in vehicles this waste heat accounts for 60 % of the fuel energy [5]. In fact, only 20 % of fuel energy is used to power the vehicle. Therefore, recovering this heat and reusing it for heating or cooling applications would significantly increase the efficiency of the engine.

TESC may also be able to increase the potential of solar energy. It can be used to eliminate the time gap between energy supply and energy demand. This is between seasons, between day-time and night-time or even between sunny and cloudy days. For instance, for space heating and domestic hot water in households and offices, the surplus of energy generated during the summer period could be stored and used in the winter, when the demand exceeds the solar supply [6,7], or, in a solar power plant, the surplus of thermal energy generated during the day could be stored and used at night or on cloudy days to produce electricity [8,9].

There are several ways to store thermal energy [10] by sensible heat [11], by latent heat [12], by sorption process (physical or chemical) or by chemical reactions. Of all these ways, chemical sorption processes (chemisorption) and chemical reactions based on solid–gas systems show the highest potential for energy savings and CO_2 emissions reduction. In both cases, heat is not stored directly as sensible or latent heat but by way of a reversible chemical process or reaction which is usually carried out in a chemical heat pump (CHP) system (closed systems).

$$S' + \text{HEAT} \Leftrightarrow S + G$$

The basic CHP system comprises a solid–gas reactor coupled with a condenser/evaporator. The working principle is illustrated in Fig. 2 in a Clausius–Clapeyron's diagram, wherein the solid–gas (S/G) and liquid–gas (L/G) equilibrium lines are given by the equation:

$$\ln(P_{eq}) = \frac{\Delta H}{RT} + \frac{\Delta S}{R}$$

The chemical heat pump system operates in two successive phases (thermal conversion) or with a time gap (thermal storage mode): charging phase (also named regeneration, decomposition or desorption) and discharging phase (also named production, synthesis or sorption). The charging phase occurs at high pressure (P_h). Heat at high temperature (T_h) is supplied to the reactor and the solid (S') decomposes. The gas (G) released from the decomposition

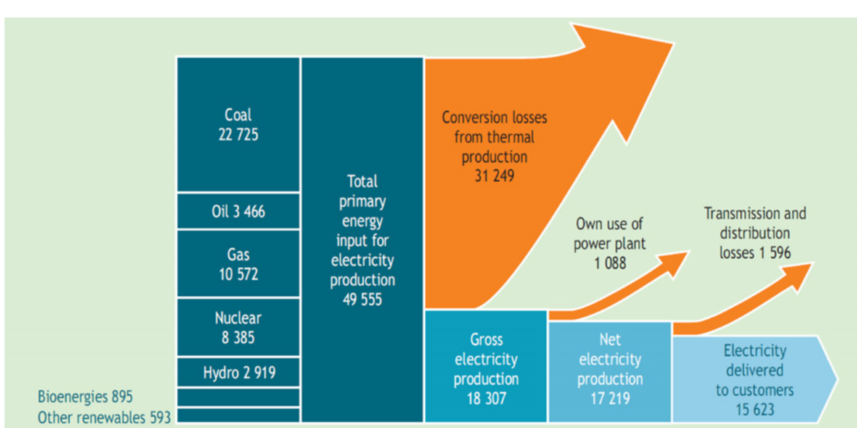


Fig. 1. Energy flows (TWh) in the global electricity system [3].

is condensed by rejecting heat from the condenser at medium temperature (T_m). By contrast the discharging phase (reverse phase) occurs at low pressure (P_l). The liquid evaporates by absorbing heat at low temperature (T_l) and the synthesis heat is released at T_m. In both phases the synthesis and decomposition occurs when the salt is removed from its equilibrium of temperature (equilibrium temperature drop, ΔT) and pressure (equilibrium pressure drop, ΔP) for heat and mass transfer [13–16].

The basic cycle shown in Fig. 2 can be used to produce refrigeration at T_l and/or to produce heat at T_m. However the two phases can be interchanged to operate the cycle as a heat transformer and thus upgrade heat from T_m to T_h. In this case the charging phase occurs at low pressure (P_l) and the discharging phase occurs at high pressure (P_h). Furthermore, in CHP systems that implies the use of non-condensable gases or that uses a condensable gas, but where the safety problem regarding the high pressure becomes an issue (legislators), the evaporator/condenser is replaced by another reactor [17–19]. In sorption processes, the CHP systems using two reactors are also known as resorption systems.

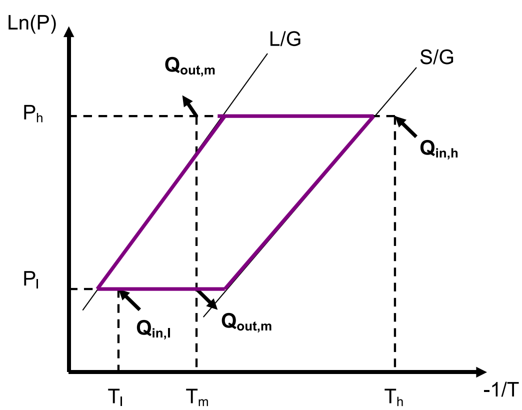


Fig. 2. Working principle of a chemical heat pump.

The advantages of chemical sorption processes and chemical reactions lie in the fact that they offer high energy density to the materials involved (important when the volume is limited), can cover a wide range of working temperatures (from −50 to over 1000 °C), and allow for long-term storage due to the negligible heat loss. Moreover, sorption and chemical heat pumps or heat transformers have several advantages to that of traditional vapor-compression heat pumps (mechanical energy). In addition to the benefit of being driven by waste heat, they utilize refrigerants with zero ozone depletion and global warming potentials, i.e. no chlorofluorocarbons (CFC) and hydrochlorofluorocarbons (HCFC), they are noise and vibration free, and long lasting [17,20].

The aim of this paper is to provide a state-of-the-art review of the experimental research on sorption processes and chemical reactions based on solid–gas systems over the last two decades. The paper gives the performances of the current materials in small and pilot scale test rigs under practical conditions.

2. Sorption processes

2.1. Description

The theory of how sorption processes work can be found in [21]. So far the chemical sorption processes studied are those between metal salts with water, ammonia, methanol or methyl-ammonia as well as metal alloys with hydrogen. Although, the processes involving methanol or methyl-ammonia have not yet been tested in prototypes under practical conditions. These processes are used to store low grade heat (< 100 °C) and medium grade heat (100–400 °C). Sorption enthalpy are typically in the range from 20 to 70 kJ mol^{-1}. Fig. 3 summarizes the reactants tested in prototypes (test rig) under practical conditions for the last two decades.

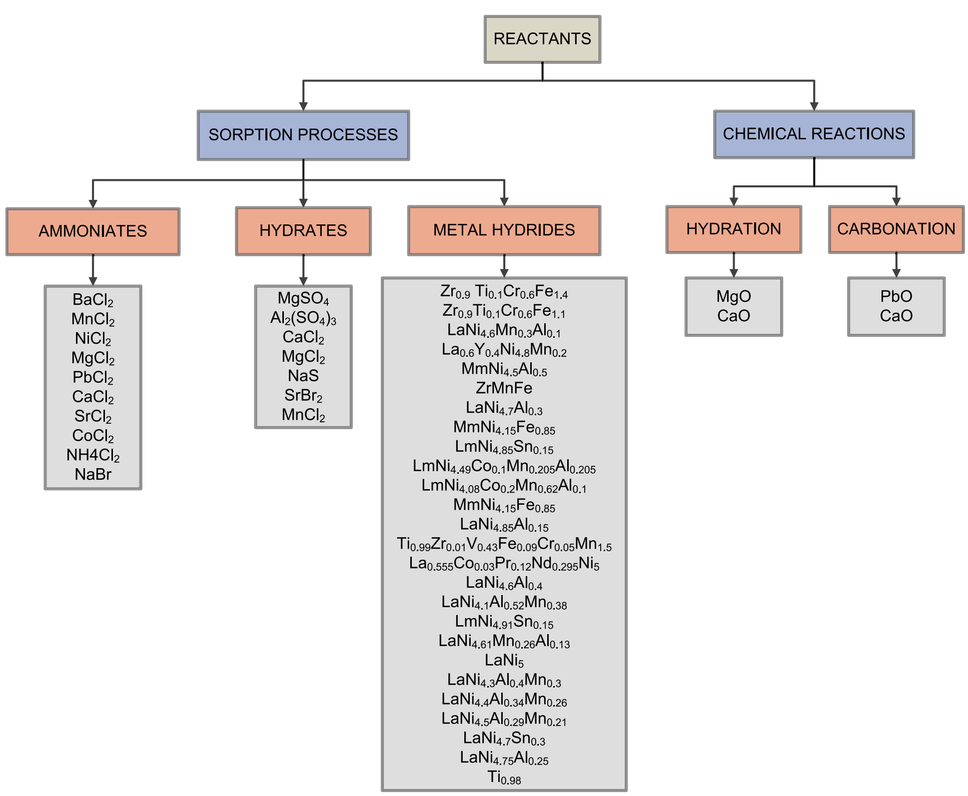


Fig. 3. Overview working pairs tested in prototypes under practical conditions.

The main target for the researchers is to develop a chemical sorption technology which can be technically feasible and economically viable, and that would be an alternative to the conventional heat pump systems. In this sense, the main research direction has been focused on finding the optimum working pair for each application and improving the performance of this technology.

Chemical sorption heat pumps based on solid–gas systems have, in general, a very low performance mainly due to the poor heat and mass transfer performance in the reactive beds (metal salts) and to the thermodynamic operation of the cycle. Poor heat and mass transfer performance in the packed bed reactor is mainly related to the low thermal conductivity of the metal salts (e.g. 0.1–0.5 $W\,m^{-1}\,K^{-1}$ for metal chlorides [22–24] and about 1 $W\,m^{-1}\,K^{-1}$ for metal hydrides [25]), the bad heat transfer between the solid bed and the reactor (heat exchanger) wall [26] and the swelling and agglomeration phenomena occurring during the sorption process with ammonia or water [27–29]. Moreover, the thermodynamic cycle operation requires large temperature swings of the sorption reactor during the process which reduces the efficiency (COP) of the system [26,30].

One way to improve the performance of the system is by improving the design of the reactor and the heat exchanger. However, over the last two decades, researchers have found on composite materials and advanced cycles concepts a new promising way to improve the low performance of the current reactants and the basic cycle.

Composite materials are mainly aimed to improve the poor heat and mass transfer performance in the reactive bed. These materials are made up by the combination of a salt hydrate and an additive with a porous structure and high thermal conductivity, which may or may not be an adsorbent, such as expanded graphite [31–38], metal foam [39–42], carbon fiber [29,43,44] or activated carbon [45]. In general, the methods used to produce composite materials are: simple mixture, impregnation, or mixture/impregnation and consolidation [46]. The degree of heat and mass transfer enhancement depends on the manufacturing method and the properties and weight fraction of the additive, as well on the reactor design [23,28]. However, experimental studies showed that composite materials can have high thermal conductivity (over 7 $W\,m^{-1}\,K^{-1}$ for consolidated composites with expanded graphite [22–24]), and can prevent or reduce agglomeration and swelling phenomena [35,45].

Advanced cycles concepts [47,48] are mainly designed to increase the efficiency and power output of the process with better heat management and mass recovery strategies. Some of the typical advanced cycle concepts include thermal wave cycle [49–51], forced convection cycle [52,53], cascading cycle [54], heat and/or mass recovery cycle [55–57], multi-effect cycle [13,15,58], sorption cycle with heat pipe thermal control [44,59] and double-way cycle [60]. However, other advanced cycles are also designed to lower the driving heat source temperature such as multi-stage cycles [61–63].

2.2. Specific reactants

2.2.1. Ammoniates

Lépinasse et al. [64–66] developed a resorption prototype for refrigeration using $BaCl_2/MnCl_2$ ammoniates pair previously mixed and compacted in expanded graphite [31]. At the operating temperatures of 195 °C/50 °C/25 °C, the reported cooling and heating power of the test rig were 1 kW (SCP=300 $W\,kg^{-1}$) and 1.3 kW (SHP=320 $W\,kg^{-1}$), respectively. These values are average values, taken from the powers measured during the 25 min of the stationary phase (from 20 % to 80 % conversion). The calculated COP was 0.35.

Li et al. [60,67,68] studied a double-effect sorption refrigeration system also using $BaCl_2/MnCl_2$ ammoniates pair but, previously impregnated in expanded graphite and consolidated in the form of cylindrical blocks. In a first study [60], the authors reported an experimental COP of 0.52 at 60 % conversion and at operating temperatures of 180 °C/30 °C/ 10 °C. In another study [67], the authors tested the same system, but using a different composition of the reactive blocks, at the operating temperatures of 180 °C/30-25 °C/10 °C. The calculated experimental COP was 0.62 at 80 % conversion. In addition, the authors reported an average SCP of 301 $W\,kg_{salt}^{-1}$, that was achieved during the 60 min of the sorption process (evaporation cooling-effect). Later, Li et al. [68] proposed a reheating process which was performed at the end of the resorption period just before the beginning of the sorption period. The $BaCl_2$ reactor was reheated by replacing the low-temperature heat transfer fluid (10 °C) with cooling water at ambient temperature (30 °C). The aim of the proposed system was to increase the equilibrium temperature drop, which increases the resorption rate and thereby the global conversion of the sorbent. At the operating temperatures of 180 °C/30-25 °C/ 10 °C, the reported experimental COP without and with reheating process was 0.57 and 0.64, respectively.

Goetz et al. [69] investigated a resorption prototype for refrigeration at 0 °C based on the ammoniates of $BaCl_2$ and $NiCl_2$ previously mixed and compacted in expanded graphite [31]. The mean cooling power during the 15 min of the refrigeration phase (~41% conversion) was 40 W (396 $W\,kg^{-1}$) at a cooling temperature of 0 °C and a heat sink temperature of 40 °C.

The ammoniates of $PbCl_2$ and $MnCl_2$ were employed by Lepinasse et al. [70] to refrigerate and keep an 88 L cold box under 0 °C during 3 h. The reactants were also mixed with expanded graphite and then compressed as described in [31]. The $PbCl_2$ reactor was placed inside the box to absorb the heat from the air, whereas the $MnCl_2$ reactor released heat to the environment. The reported cooling capacity of the resorption refrigerator was 48 $kWh\,m^{-3}$.

Recently, Bao et al. [71,72] also investigated a resorption refrigerator for simultaneously cooling the upper section of a 33 L storage box at 0 °C to 6 °C and freezing the bottom section at −16 °C to −14.5 °C. The ammoniates pair used was $NH_4Cl/MnCl_2$, previously impregnated in expanded graphite and consolidated in the form of cylindrical blocks according to [34,36]. The experiments were carried out at different ambient air box temperatures ranging from 20 to 35 °C. Depending upon initial air box temperature, the air in the bottom section reached the minimal value of −16 to −14 °C and kept below −10 °C for about 3 h and, the upper section could be cooled down to −1–6 °C. The average SCP in 3 h operation was 43 $W\,kg_{salt}^{-1}$. However, the average effective cooling power ranged from 11 $W\cdot kg_{salt}^{-1}$ at an ambient air box temperature of 35 °C to 18 $W\,kg_{salt}^{-1}$ at a ambient air box temperature of 20 °C.

Also an $NH_4Cl/MnCl_2$ resorption system was studied for simultaneously heat and cold production by Xu et al. [73]. Consolidated composite materials made of the reactive salt and expanded graphite were used as the reactive medium [36]. At the operating conditions of 140 °C/30–75 °C/0 °C, the specific cooling power was 1.2 $MJ\,kg^{-1}\,day^{-1}$, the COP was 0.35 and the COPA was 1.3.

Oliveira et al. [74] studied a sorption system using NaBr with NH_3 for air conditioning applications and a resorption system using NaBr and $MnCl_2$ with NH_3 for simultaneous heating and cooling. The salts were impregnated in expanded graphite and consolidated in the form of cylindrical blocks following a procedure described by Oliveira et al. [36]. In the air conditioning system, the authors reported a specific cooling capacity of $129\pm7\,W\cdot kg^{-1}$ and a COP of 0.46 ± 0.01 for 40 min process

and at the operating temperatures of 65 °C/30 °C/15 °C. On the other hand, in the resorption system the COP reached a value of 0.21 and the COPA was 1.11 at the operating temperatures of 165 °C/30–70 °C/10 °C.

A heat transformer resorption system based on the $CaCl_2$ and $MnCl_2$ salts was investigated by Wang et al. [75]. In addition, the authors studied the influence of a gas valve control on the performance of the heat transformer. The reactants were also impregnated in expanded graphite and consolidated in the form of cylindrical blocks by a methodology disclosed by Zhang et al. [32]. At the operating temperature of 150 °C/120 °C/40 °C, the reported SHP and COP were 235 W kg^{-1} and 0.22, respectively. Further, the addition of a gas valve control improved by 6 % the SHP and by 14 % the experimental COP.

Llobet and Goetz [76] proposed a double-effect sorption process system for cooling applications with heat recovery by direct contact with the reactors. The selected working pairs for the process were the ammoniates of $SrCl_2$ and $CoCl_2$, previously mixed and compacted in expanded graphite [31]. The authors claimed that the double effect by direct contact allows to consider high energetic performances, a simple working mode and a compact installation. At the operating temperatures of 240 °C/7.5 °C/−4 °C, the reported SCP and COP were 145 W kg_{salt}^{-1} and 0.25, respectively. In addition, the authors compared the results of the current system with the previous experimental results obtained by Nevau et al. [77] and Wagner [78] in two different types of double-effect system. Nevau et al. [77] studied a double-effect system using $MnCl_2$ and $NiCl_2$ salts. At the operating temperatures of 280 °C/10 °C/−5 °C, the reported SCP and COP were 29 W kg_{salt}^{-1} and 0.21, respectively. On the other hand, Wagner [78] investigated a double effect system controlled by heat pipes using $SrBr_2$ and $NiCl_2$ salts. At the operating temperatures of 340 °C/8 °C/−4 °C, the reported SCP and COP were 134 W · kg_{salt}^{-1} and 0.38, respectively.

A resorption heat transformer based on the ammoniates of $MgCl_2$ and LiCl was first studied by Haije et al. [39] and followed by van der Paal et al. [42,79]. The target of the system was to upgrade the waste heat from a temperature level between 100 to 150 °C to a temperature level between 180 to 220 °C and thus to produce medium pressure steam. Haije et al. [39] developed a resorption prototype based on a novel concept of "tube-hollow-fin" heat exchanger to increase heat transfer. In addition, the ammoniates were impregnated in metal foam. At the operating temperatures of 200 °C/155-200 °C/20 °C, the authors reported a mean power output of 0.4 kW (about 222 W kg^{-1} of salt) during the 40 min of the heat production period and an experimental COP of 0.11. The poor performance of the system was attributed to the poor stability and mass transfer limitations of the salts in the metal foam [39,42]. Later, van der Paal et al. [42] developed a new method for the impregnation of the salts in metal foam and designed a shell and tube heat exchanger type of reactor for the prototype. The temperature of the LiCl reactor was varied between 20 °C and 80 °C for the $MgCl_2$ reactor at 130 °C and between 20 °C and 130 °C for $MgCl_2$ reactor at 180 °C and 200 °C. The authors found that only 40 % of the $MgCl_2 \cdot 2NH_3$ absorbed ammonia to form $MgCl_2 \cdot 6NH_3$, which was attributed to the short cycle time (1 h). The system was stable for at least the 100 cycles performed with an average heat in/output of about 300 W and a peak power in/output of about 600 W. Finally, the calculated COP was close to 0. The low value was also attributed to the large thermal mass of the reactor. In a recent study [79], the absorption of ammonia by $LiCl \cdot NH_3$ with an ammonia pressure of 540 kPa was studied at 50 °C. The authors found that only 36 % of the theoretically available amount of ammonia was absorbed in the 10 cycles performed. Furthermore, the authors observed the formation of the liquid phase at this pressure. This phase change was also found in a previous study [80].

A sorption refrigeration system using $CaCl_2$ impregnated in expanded graphite and consolidated in the form of cylindrical blocks was studied by Oliveira et al. [35,36]. In a first study [35], the authors obtained the highest average SCP of 255 W kg^{-1} at the synthesis time of 40 min and at the operating temperature of 97 °C/30 °C/−18.3 °C. At this moment, the overall conversion was 48 % and the evaporation temperature dropped to −22 °C. The average SCP measured for the whole process was 194 W kg^{-1} (140 min). In a later study [36], the manufacturing conditions and composition of the reactive blocks differed from that of the previous study [35]. The authors obtained a SCP and cooling power density above 1000 W · kg_{salt}^{-1} and 290 kW m^{-3}, when the evaporation temperature was in the range from -20 °C to -10 °C (typical temperatures for ice production), and the heat sink temperature was in the range from 20 °C to 30 °C. The calculated COP was 0.35 when the consumed mass of NH_3 was 0.8 kg_{salt}^{-1} (87 % conversion, $CaCl_2 \cdot 2NH_3$ to $CaCl_2 \cdot 6NH_3$).

Wang et al. [81] studied a double-sorption ice maker driven by the exhaust gas of the diesel engine from fishing boats and cooled by seawater (heat sink). The reactive composite material was made from $CaCl_2$ and activated carbon, and cement as a binder, following a method described by Wang et al. [45]. The two sorption reactors were of tubular type (Fig. 4), wherein the composite material was filled and pressed between fins of the finned tubes and the inside of the finned tubes served as the heat pipe part in the sorption reactor. Further, the sorption cycle included a mass recovery process to improve the system performance. At the optimum cycle time of 50 min, the optimum mass recovery time of 47 s and the operating temperatures of about 100 °C/25 °C/−15 °C, the authors reported an average cooling capacity of 1.37 kW, a COP of 0.41 and a SCP of 731 W kg_{salt}^{-1}. In addition, the mass recovery process improved the COP and SCP by 15.5 % and 24.1%, respectively. Lu et al. [82] performed further experiments on the same prototype but including, besides a mass recovery process, a heat recovery process in the sorption cycle. The authors obtained an average SCP of 676.8 W kg_{salt}^{-1} and a COP of 0.34 when the operating temperatures were 114 °C/25 °C/−20 °C, the cycle time was 70 min, the mass recovery time was 40 s and the heat recovery time was 2 min. In addition, the performance of the double-sorption ice maker was investigated when it was powered by solar water heating but without including a heat recovery process in the sorption cycle. When the cycle time was 24 min, the mass recovery time was 40 s and the operating temperatures were 80 °C/30 °C/−15 °C, the reported average SCP and COP were 161.2 W kg_{salt}^{-1} and 0.12, respectively.

Later, Lu et al. [83] redesigned the main components of the double-sorption ice maker to improve the performance of the system (Fig. 5). The authors reported an average SCP of 369.1 W · kg_{salt}^{-1} and a COP of 0.2, at the operating temperatures of 126 °C/22 °C/−7.5 °C and, the heat and mass recovery time of 2 min and 40 s, respectively. In a further study, Li et al. [84] tested the prototype with the implementation of a novel heat and mass recovery process with heating the high temperature reactor (desorption) and cooling the low temperature reactor (sorption) during the mass recovery process. The authors obtained an average SCP of 486.5 W kg_{salt}^{-1} and a COP of 0.27 at the operating temperatures of 160 °C/10 °C/−19 °C, at the half-cycle time of 17 min and the optimum heat and mass recovery time of 120 s and 40 s, respectively. According to the authors, the novel heat and mass recovery process improved the SCP by 18.9 % and COP by 17.4 %, if compared with the conventional heat and mass recovery process. In a later study, Li et al. [85] proposed a two-stage heat recovery process to reduce the heat source temperature and improve the performance of the conventional two-stage process. At the operating temperatures of 103 °C/ 30°C/ −19.7°C, the reported average SCP was 228.4 W kg_{salt}^{-1} and COP was

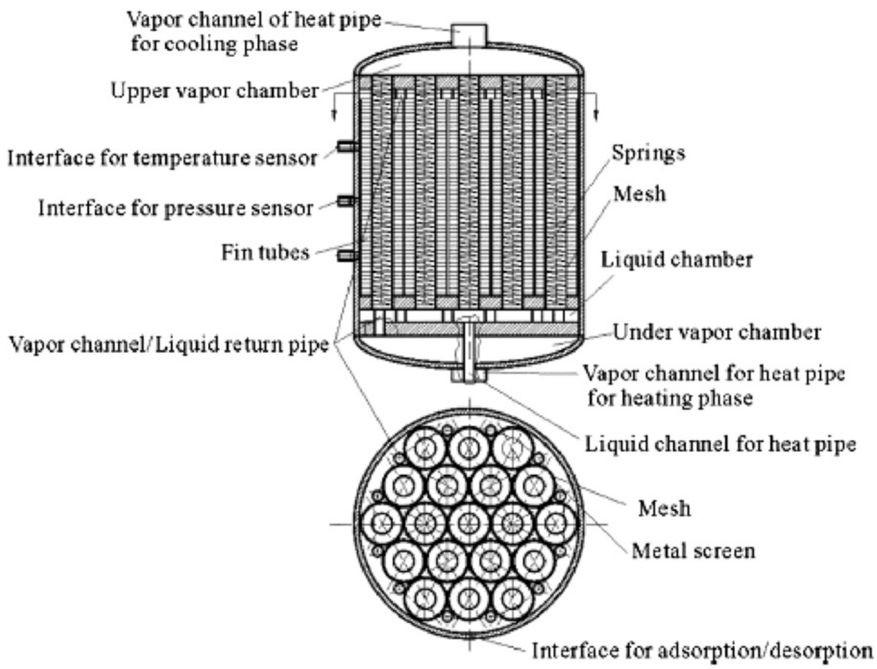


Fig. 4. Design of the sorption reactor [80].



Fig. 5. Double-sorption ice maker prototype [82].

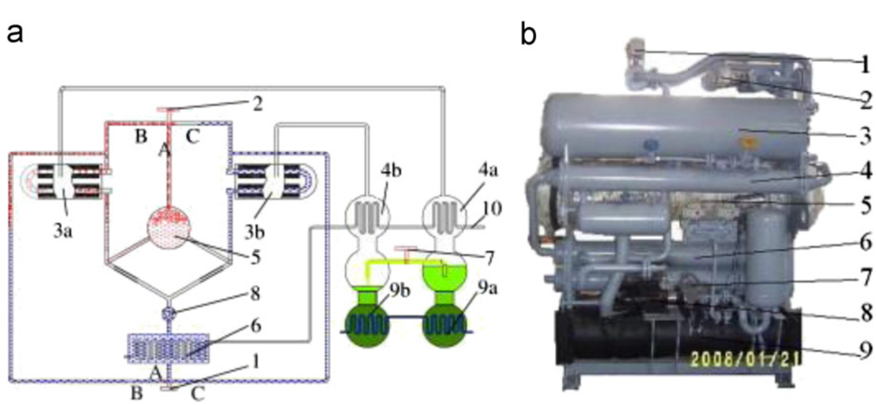


Fig. 6. Structure of refrigerator. (A) Schematic diagram. (B) Photo of refrigerator. (1) water valve, (2) vapor valve, (3) sorption reactors, (4) condensers, (5) vaporgenerator, (6) cooler, (7) ammonia valve, (8) pump, (9) evaporators and (10) cooling water [86].

0.14. Moreover, the performance of the two-stage heat recovery cycle was improved by more than 23 % when compared with the conventional two-stage cycle under the same operating temperatures.

Xia et al. [86] and recently, Li et al. [87] also tested a double-sorption ice maker with mass recovery process, however using the consolidated composite material made of expanded graphite and impregnated with $CaCl_2$. Furthermore, the authors stressed that the new prototype (Fig. 6) was designed with only 3 valves, which increased the reliability of the system when compared with the previous prototypes (185–189) having more than 7 valves. Xia et al. [86] reported a cooling power of 8.4 kW with an average SCP of 302.7 W kg_{salt}^{-1} and COP of 0.32 at the operating temperatures 110 °C/25 °C/-15 °C, the optimum cycle time of 25 min and the mass recovery time of 45 s. On the other hand, Li et al. [87] tested the system under the same operating condition but at a higher heat source temperature of about 140 °C. The reported cooling power, average SCP and COP were 11.4 kW, 422.2 W kg_{salt}^{-1}, and 0.27, respectively.

A solar-assisted sorption drier based on the ammoniated of $CaCl_2$ was designed and tested by Fadhel et al. [88] and Ibrahim et al. [89,90]. The sorption reactor was of shell and tube heat exchanger, wherein the reactant was placed between the fins of the heat exchanger. The incoming air was heated by condensation of ammonia during the desorption process and was entered into the drying chamber to dry lemon grass. Part of the moist air stream produced after the drying process was diverted through the evaporator, where it was cooled. Dehumidification took place as the heat was given by the evaporation of ammonia and consequent sorption of $CaCl_2 \cdot 2NH_3$. The air was then passed through the condenser again, where it was reheated by the ammonia condensation and then entered to the drying chamber. The performance of the system was evaluated over 9 h (drying time, 8 am–17 pm) on a clear and on a cloudy December day in Malaysia. The authors reported maximum heating performance of 2 on a clear day and of 1.4 on a cloudy day for the integrated chemical heat pump with solar collector and storage tank. Furthermore, the total energy output on a clear day was 51 kWh and on a cloudy day was 25 kWh.

Vasiliev et al. [91] investigated a sorption refrigerator system using also $CaCl_2$ but impregnated in "Busoft" (carbon fibers). These composite materials were suggested due to their stability, low cost and suitable temperature range. The experiments were carried out in a cylindrical reactor using an inner heat pipe as the heat exchanger. Metal fins were fixed on the heat transfer surface to increase the heat transfer between the reactive bed and the heat pipe envelope. At the operating temperatures of 120 °C/ 50°C/−18°C and the cycle time of 25–30 min, the calculated COP was close to 0.43.

Vasiliev et al. [91] also studied a resorption heat pump using the ammoniates of $BaCl_2$ and $NiCl_2$ impregnated in "Busofit" for simultaneous heat generation (steam at Tm = 120–130 °C) and chilled water production (Tl = 3–5 °C). The high heat temperature source was about 240 °C. A similar type of reactor as previously described was used for the experiments. The authors obtained an experimental COP of more than 0.44, while the COA was 1.44. Vasiliev et al. [92,93] also performed experiments with two resorption heat pumps to allow a continuous operation. The experiments were performed using the ammoniates of $BaCl_2$ and $MnCl_2$ impregnated in "Busofit". The authors reported a power output of 350 W per kg of composite for 30 min operation.

Further studies by Vasiliev et al. [93–95] were carried out in a three-bed double-effect sorption heat pump to ensure the regime of continuous heat and cold supply in the presence of two independent refrigerating sources. The three reactants used were $BaCl_2$, $NiCl_2$ and $MnCl_2$ impregnated in "Busofit". Two prototypes with different working principle were built. However, in the first prototype, the sorption reactor of $MnCl_2$, $NiCl_2$ and $BaCl_2$ were desorbed at 230 °C, 180 °C, and 90 °C, respectively by the waste gases of the internal combustion engine and by the hot liquid from the cooling liquid system of the engine. The experimental COP obtained in this prototype was 0.42. In the second prototype desorption was carried first in the $MnCl_2$ and $NiCl_2$ reactor at 450–500 °C by the waste gases and then in the $BaCl_2$ reactor at 95 °C following a procedure described in [95]. The experimental COP obtained in the second prototype was 0.62.

Le Pierrès et al. [96,97] investigated a two cascade sorption refrigeration prototype using $BaCl_2$ as the reactive salt pair previously mixed and compacted in expanded graphite [31]. The purpose of this study was to cool down a 560 L insulated cold box to about −25 °C using only low grade heat produced by two simple flat plate solar collectors (Fig. 7). Desorption process was carried out during the day time and sorption process (refrigeration) was carried out during the nighttime. The experiments were performed in Perpignan (France) from 24 May to 28 July 2005 and from 9 September to 10 October 2005. The authors concluded that the capability of the process to produce deep-freezing temperatures

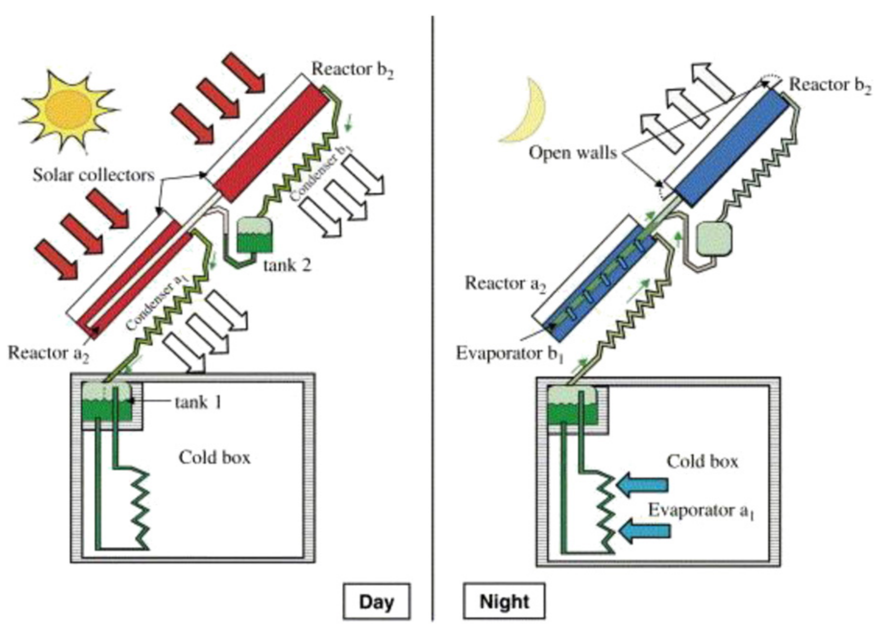


Fig. 7. Simplified scheme of the prototype during the regeneration and cold production phases [96].

was mainly influenced by the solar irradiation and the environment temperature. The lowest temperature reached in the evaporator from the cold box was −31 °C. Temperatures lower than −20 °C were achieved mainly when the solar irradiation was higher than 18 MJ m^{-2} day^{-1} and during 72 % of nights. The cold box temperatures were always between 3 °C and 6 °C higher than those of the evaporator. Moreover, the average COP during the 93 days of experiments was 0.031.

Chen et al. [98] studied a consolidated composite material made of $BaCl_2$ impregnated with expanded graphite to be used in a solar assisted sorption air conditioner. The values of COP and average specific cooling power reached 0.5 and 192 W kg^{-1}, at the operating temperatures of 80 °C/30 °C/15 °C.

Rivera et al. [99] investigated the feasibility to operate a $BaCl_2$ sorption refrigerator system with low cost solar flat plate collectors. The authors found that it was possible to generate ammonia vapor at 53 °C using hot water at 70 °C as heat source temperature, while keeping the condenser at 23 °C. In addition, the system produced cold at temperatures below 0 °C for about 1.5–2 h.

Kiplagat et al. [100] proposed a consolidated composite material made of expanded graphite impregnated with LiCl salt to be used in solar assisted sorption ice maker. The salt was impregnated into the expanded graphite according to the methodology given by [35]. The authors obtained the highest average SCP of 117 W kg^{-1} and a COP of 0.47 at the operating temperatures 80 °C/25 °C/−5°C and 30 min of refrigeration time.

Chen et al. [101] studied a consolidated material made of $SrCl_2$ impregnated in expanded graphite to also be used in a solar assisted sorption ice maker. The calculated average specific cooling power and COP of solar ice making chemical heat pump was 738 W kg^{-1} and 0.435, respectively.

Cerknenik et al. [102] investigated a double sorption reactor working in counter-phase that uses the ammoniate of $NiCl_2$ as the reactant. The device was tested as part of a cascading triple-effect sorption device, to increase the COP of the cooling system. The cascade cooling device was based on coupling a double-effect LiBr–H_2O cooling device as the bottom part of the cascade with the $NiCl_2$ sorption cooling device as the top part of the cascade. The $NiCl_2$ sorption cooling device can be used at higher temperatures (above 200 °C) at which efficient absorption devices cannot be used. The sorption reactors were of tubular type. An evaporator heat pipe was placed in the middle part of each tube. The rest was filled with the ammoniate of $NiCl_2$ previously impregnated in expanded graphite and compressed. The desorption process temperature was 300 °C and the sorption process temperature was 200 °C. The condensation ammonia pressure was about 1000 kPa and the evaporation ammonia pressure was about 450 kPa. The reported, average calculated COP was about 0.17.

Aidoun and Ternan [43,103] investigated a sorption system using $CoCl_2$ impregnated on carbon fibers for heating and cooling in the food processing industry. The experiments were carried out in a cylindrical packed bed reactor. In addition, the reactor was weighed continuously during the experiments, thereby providing an instantaneous measurement of the reaction rate that was independent of the heat transfer measurements. The first study [43] was focused on the decomposition process. The power densities measured during the decomposition reaction had values of 280 kW m^{-3} sustained for 30 min when the decomposition pressure was set to 1000 kPa and the condenser temperature was kept at 5 °C. In addition, it was observed that there was a threshold temperature (≥ 300 °C) beyond which salt degradation occurred as previously showed in [104,105]. The second study [103] was focused on the sorption process. The authors reported a peak power output of about 235 kW m^{-3}, when the evaporator pressure was kept in the range of 700–795 kPa and the pressure control valve set to maintain the reactor at a constant pressure of approximately 450 kPa.

2.2.2. Hydrates

The hydrates of $MgSO_4$, $MgCl_2$, $CaCl_2$, and $Al_2(SO_4)_3$ were proposed for seasonal heat storage of solar energy in the built environment by Essen et al. [6,106]. The authors aimed to store the surplus of solar energy generated during the summer and meet the heating demand for space heating and domestic hot water during the winter, when the demand exceeds the solar supply. The materials were tested under practical conditions at 150°C/10-50°C/10°C, where 150 °C was the assumed maximum temperature that can be delivered by a medium temperature collector (vacuum tube) during the summer period and 10 °C was the assumed temperature of the borehole heat exchanger connected to the evaporator/condenser. The performance of the material was assessed by measuring the temperature lift of the bed during the sorption process. The $MgCl_2$ reached a maximum temperature lift of 19 °C while the $CaCl_2$, the $MgSO_4$, and the $Al_2(SO_4)_3$ reached a maximum temperature lift of 11 °C, 4 °C and 1 °C, respectively. However, the $MgCl_2$ and $CaCl_2$ tend to form a gel-like material during the sorption process due to their hydroscopic nature.

Following the same research line, Zondag et al. [107] further investigated the $MgCl_2$ under practical conditions. In this case, however, the experiments were performed in an open system (atmospheric) instead of the close system used in the previous study [106]. This choice was based on a previous techno-economical study done by Zondag et al. [108], which had shown that these systems were more economical and reliable. The authors found that HCl was formed during the dehydration of $MgCl_2 \cdot 7H_2O$ at temperatures above 135 °C. The formation of this gas not only degrades the storage material, but it is also strongly corrosive. Therefore, dehydration was limited to a temperature below 135 °C. In addition, the over-hydration of $MgCl_2$ was avoided by impregnation into a carrier material (cellulose). The hydration experiments were performed using a moistened nitrogen flow of 20 slpm with a vapor pressure of 1.2 kPa and at an initial bed temperature of 25 °C. The measured temperature lift was 15 °C and a significant temperature rise was maintained in the bed after 24 h. The calculated energy density of the material after 23 h hydration was 0.14 MJ kg^{-1}.

De Boer et al. [109] tested a sorption cooling system using Na_2S for residential and industrial applications. A spiro-tube heat exchanger was used as reactor. Because the Na_2S–H_2O system has a eutectic melting point at 83 °C, the upper limit for the condensation temperature was fixed at about 27 °C. Nevertheless, the Na_2S was impregnated on fibrous cellulose to allow partial melting of the material without significant irreversibility [7]. Peak cooling powers of 500 to 700 W were measured at evaporation temperatures of 10 to 15 °C, which remained relatively constant until all the water was evaporated. The measured maximum thermal storage capacities of the prototype were 3.2 kWh for heat and 2.1 kWh for cold. Finally, the reported COP was 0.57.

Stitou et al. [110] developed a sorption system using $MnCl_2$ previously mixed with expanded graphite and compacted according to [31,33,34]. The purpose of the system was to produce heat at a temperature level suitable for industrial purposes (typically 160 °C) from waste heat at 90 °C (high pressure mode) or from environment at 35 °C (low pressure mode). The experimental reactors were surrounded by gravitational heat pipes for heat recovery during the sorption period. The prototype was experimentally evaluated for the high pressure mode at different working temperatures (320–330 °C, heat source; 120–145 °C, condenser; 145–160 °C, heat sink; 95 °C, evaporator). The total cycle time was about 87 min and the average powers were 1290 W for the heating and desorption, 1790 W for cooling and sorption, 530 W for the condenser and 560 W for the evaporator. The mean value of the COA was 1.25.

A solar assisted sorption system using $SrBr_2$ was tested by Lahmidi et al. [111]. The system was designed for heating floor in winter or mid-season at 35 °C and refreshing floor in summer at 18 °C. $SrBr_2$ was mixed with expanded graphite and compacted according to a methodology described by Mauran et al. [34]. The reported mean cooling power was 48 $kW \cdot m^{-3}$ at the operating temperatures of 80 °C/35 °C/18 °C (summer) whereas the heating power in winter was 36 kW m^{-3} at the operating temperatures of 70 °C/35 °C/12 °C (winter). The average powers were calculated from the experimental measurements obtained between 0 to 90 % of conversion. Based on previous results, Mauran et al. [112] built a prototype reactor that was able to store, with a complete reaction, 60 kWh and 40 kWh for heating and cooling respectively. In summer conditions (66 °C/35–30 °C/18 °C), the mean refreshing power was −2.6 kW during the 14 h of the sorption period (0–92 %). On the other hand, in mid-summer conditions (70 °C/12-30 °C/12 °C), the mean heating power was 2.2 kW during the first half of the sorption process (55 % conversion).

2.2.3. Metal-hydrides

Lee et al. [113] studied a resorption metal hydride air conditioner using $Zr_{0.9}Ti_{0.1}Cr_{0.6}Fe_{1.4}/Zr_{0.9}Ti_{0.1}Cr_{0.9}Fe_{1.1}$ pair which was driven by waste heat exhausted from automobile and industrial plants. The reactors used were of tubular type. Aluminum fins were installed at the outer part of the tube to improve the heat transfer characteristics between the air and the reactor surface. At the inner part of the reactor, mesh brass screens were used as metallic structure to enhance the heat transfer rate in the hydride bed. At the operating temperature of 220 °C/30 °C/18 °C, 4 min heating time and 7 min cooling time, the maximum reported SCP was about 151 W per kg of total hydride mass (271 W per kg of desorbing metal hydride).

A solar assisted resorption refrigerator system based on $La_{0.6}Y_{0.4}Ni_{4.8}Mn_{0.2}/LaNi_{4.6}Mn_{0.3}Al_{0.1}$ pair was investigated by Imoto et al. [114]. At the operating temperatures of 140 °C/20 °C/−20 °C and half-cycle time of 19 min (80 % conversion), the reported thermal power and COP were 1860 W and 0.42, respectively.

Ram Gopal and Srinivasa Murthy [115] carried out experimental studies on a resorption cooling system working with $MmNi_{4.5}Al_{0.5}$/ZrMnFe pair. The metal hydride cooling system consisted of two identical reactors in shape and size which were of tube and coil-type. The authors investigated the performance of the heat pump at different half-cycle times (3–12 min) and different operating temperatures (T_h=110–130 °C, T_m=25–30°C, T_l= 5–15 °C). Depending upon the operating conditions, the specific cooling power was found to lie between 30 and 45 W per kg of total hydride mass (60 to 90 W per kg of desorbing hydride) and the COP varied from 0.2 to 0.35.

Chernikov et al. [116] investigated a resorption system using $MmNi_{4.15}Fe_{0.85}/LaNi_{4.6}Al_{0.4}$ pair for simultaneous production of chilled water (< 4°C), and domestic and industrial hot water (50 °C). The experimental test rig was based on a modular principle, each module containing the high-temperature and the low-temperature metal hydrides which were separated by a collector filter for hydrogen transfer. In addition, corrugated aluminum foil was used to increase the heat transfer rate in the hydride bed. The regeneration process was carried out by heating the high-temperature part to 200 °C. Cooling water at 10.1 °C was used as the heat sink. The volume of the tank with heat insulation for the collection of chilled water was 18 l and the reference temperature of the water was 21.1 °C. The system was operated during 8 half-cycles of 20 min each. At the previous conditions, the average cooling power was 154 W with an output temperature of the chilled water of 1.5 °C. The total heat consumption and cold production were 12.6 MJ and 1.48 MJ, respectively.

A resorption system using $MmNi_{4.15}Fe_{0.85}/LaNi_{4.7}Al_{0.3}$ was investigated by Kang et al. [117]. The reactors were of finned tube type. At the operating conditions of 150 °C/30 °C/20 °C and 20 min cycle time, the reported COP was about 0.2.

Willers and Groll [118] designed and tested a two-stage metal hydride heat transformer using $LmNi_{4.85}Sn_{0.15}$ (A), $LmNi_{4.49}Co_{0.1}Mn_{0.205}Al_{0.205}$ (B) and $LmNi_{4.08}Co_{0.2}Mn_{0.62}Al_{0.1}$ (C). The heat transformer comprised three pairs of reactors (A1/2, B1/2, C1/2) interconnected in a special "star"-scheme (Fig. 8, scheme 2).

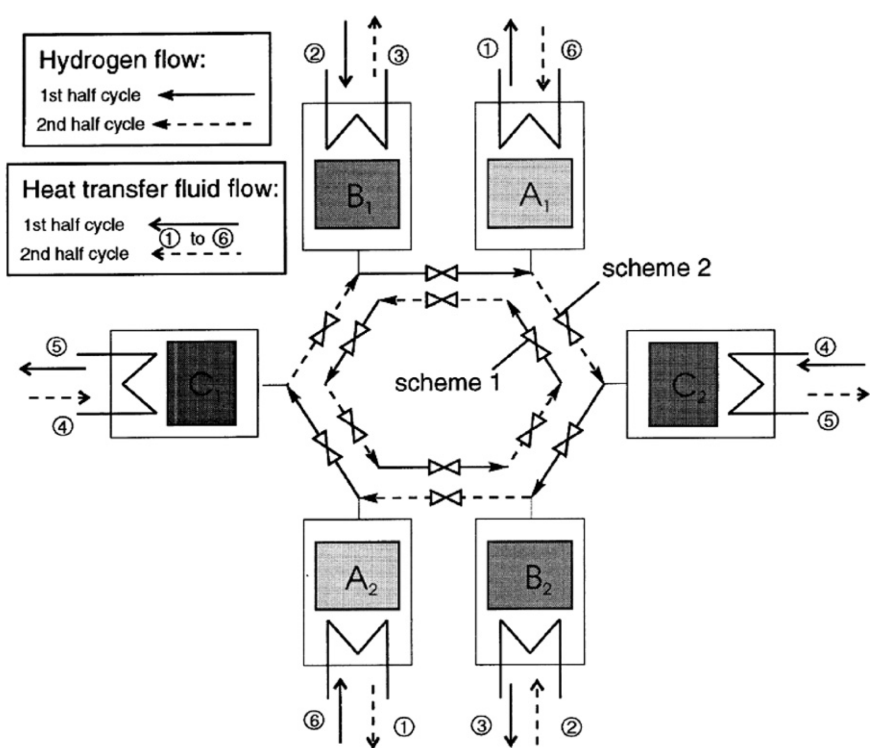


Fig. 8. Working principle of the two-stage metal hydride heat transformer [118].

The useful heat was generated at T_h by the hydrogen absorption in hydride C1, which absorbed hydrogen released from hydride A2 at the driving temperature T_d. Hydride C2 was desorbed at T_d and the released hydrogen was absorbed in hydride B2. Finally, hydrogen flowed from B1 to A1 by desorption of B1 at T_d. Driving heat at temperature level T_d must be supplied three times, while useful heat $Q_{useful,C}$ is generated only once. After the first half cycle, the gas valves were closed an internal heat recovery could take place between A1 and A2, B1 and B2, and C1 and C2. The theoretical COP was about 1/3, if thermal masses are neglected. Each hydride reactor consisted of two units containing a tube bundle of seven cylindrical reactors beds filled with the respective metal hydride and arranged in a hexagonal structure (Fig. 9). To increase the thermal conductivity of the bed, a helical copper band (Fig. 10), which is helically soldered into the reactor, was used as heat conduction matrix. At the operating conditions of 190 °C/130 °C/40 °C ($T_h/T_d/T_c$), the power output was about 7 kW which corresponded to a cycle time of about 20 min, i.e. 10 min for each cycle time.



Fig. 9. Opened reactor unit [118].



Fig. 10. Reaction bed with a copper band as heat conduction matrix [118].

Klein et al. [40] investigated experimentally a two-stage metal hydride system with $LmNi_{4.91}Sn_{0.15}$, $LaNi_{4.1}Al_{0.52}Mn_{0.38}$ and $Ti_{0.99}Zr_{0.01}V_{0.43}Fe_{0.09}Cr_{0.05}Mn_{1.5}$ in a cascading system as a topping cycle together with a double-effect lithium bromide/water system as the bottoming cycle. The system comprised six reactors also interconnected in a "star" scheme but following a different working principle. In the first half-cycle hydride C1 was desorbed at T_d and the released hydrogen was absorbed in hydride A1 at T_m. Heat for the bottoming cycle was generated at T_h by the hydrogen absorption in hydride C2 which absorbed hydrogen released from hydride B2 at the driving temperature T_d. Finally, hydrogen flowed from A2 to B1 by desorption of A2 at T_c (useful cold). After the first half cycle, the gas valves were closed and internal heat recovery could take place between A1 and A2, B1 and B2, and C1 and C2. Each hydride reactor consisted of four reaction beds. Further the hydride powder was contained in Aluminum-foam cylinders to improve heat and mass transfer (Fig. 11). The average cooling power of the system was about 970 W while the heating power for driving the bottoming cycle of the cascade was 1.63 kW. The cooling temperatures were in the range from 2 to 16 °C (T_c), a heat sink temperature of 23 °C (T_m), a temperature of the heat transferred to the bottoming cycle of 100 °C (T_h) and a heat driving temperature of 330 °C (T_d). The coefficient of performance for cooling was of 0.51 and for heat amplification of 0.86

Qin et al. [120] developed a metal hydride resorption air conditioner using the $La_{0.6}Y_{0.4}Ni_{4.8}Mn_{0.2}$/ $LaNi_{4.61}Mn_{0.26}Al_{0.13}$ pair which was driven by the exhaust heat of an automobile engine. The experimental test rig was composed of two pair of reactors to produce a quasi-continuous cold output. The operating temperatures were 150 °C/30 °C/0 °C and the operating times were 800 s for pre-heating, 850 s for regeneration, 650 s for pre-cooling and



Fig. 11. Cross-section of a reaction bed [119].

1300 s for refrigeration. The maximum cooling power was 639 W, which was achieved at the beginning of the refrigeration period, while the average cooling power of this period was 238 W. The average cooling power of the whole cycle was 84.6 W and the cooling power per alloy was 7.7 W kg^{-1} (15.4 W per kg of desorbing alloy). Moreover, the reported COP was 0.26.

Ni et al. [121] also tested a quasi-continuous metal hydride resorption air conditioner using the $La_{0.6}Y_{0.4}Ni_{4.8}Mn_{0.2}/LaNi_{4.61}Mn_{0.26}Al_{0.13}$ pair. The system was also driven by the exhaust heat of an automobile engine. At the operating temperatures of 150 °C/30-32 °C/20 °C, the reported lowest refrigeration temperature, average cooling power and COP were 1.9 °C, 244.23 W and 0.30, respectively.

Linder et al. [122] presented a resorption system using the $Ti_{0.99}Zr_{0.01}V_{0.43}Fe_{0.09}Cr_{0.05}Mn_{1.5}/LmNi_{4.91}Sn_{0.15}$ pair for automotive cooling. The experiments were carried out using two capillary tube bundle reaction bed (Fig. 12) due to its large heat transfer surface and consequently expected short cycle times. At the operating temperatures of 130 °C/28 °C/20 °C and at the optimum half-cycle time of about 100–120 s, the calculated specific cooling power was about 780 W per kilogram desorbing metal hydride.

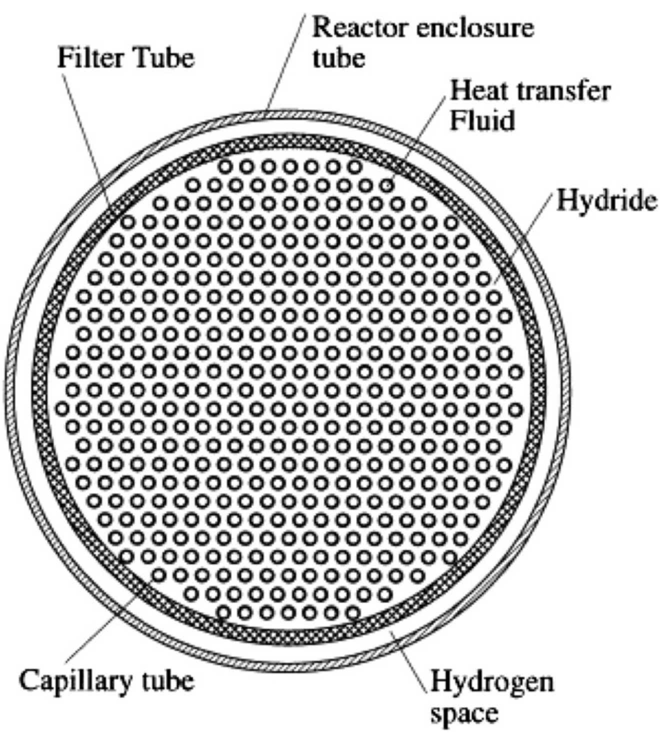


Fig. 12. Cross-section of a capillary tube bundle reaction bed [123].

A multi-hydride thermal wave device for simultaneous heating and cooling was investigated by Willers et al [41]. The process flow diagram and the thermodynamic cycle of the device are illustrated on a Van't Hoff plot in Fig. 13. The system employed nine different metal hydrides: $LaNi_{4.3}Al_{0.4}Mn_{0.3}$ (1), $LaNi_{4.4}Al_{0.34}Mn_{0.26}$ (2), $LaNi_{4.5}Al_{0.29}Mn_{0.21}$ (3), $LaNi_{4.7}Sn_{0.3}$ (4), $LaNi_{4.75}Al_{0.25}$ (5), $LaNi_{4.85}Al_{0.15}$ (6), $LaNi_5$ (7), $La_{0.555}Co_{0.03}Pr_{0.12}Nd_{0.295}Ni_5$ (8) and $Ti_{0.98}$ (9). The prototype consisted of 4 reactors (HT1, HT2, LT1 and LT2) and each reactor had three reaction beds. The HT reaction beds were filled with metal hydrides 1 to 7 and the LT reaction beds with metal hydrides 8 and 9. Moreover, the hydride powder was contained in aluminum-foam cylinders to improve heat and mass transfer (Fig. 11). The experiments were performed at 235 °C/23 °C/18 °C and with 60 % of the maximum hydrogen capacity. The overall time was 1500 s. The authors obtained a cooling power in the range of 230 W (outlet temperature 10 °C) to 500 W (outlet temperature 0 °C) with an average of 360 W. The COP during the cold generation period (550 s) was about 0.6 for cooling and 0.33 for the complete cycle.

3. Chemical Reactions

3.1. Description

The basic theory of thermal energy storage and conversion by chemical reaction can be found in [18,125]. Over the last two decades, the experimental research on chemical reactions has been focused on the hydration and carbonation of metal oxides. These reactions are used to store medium and high grade heat (> 400 °C). The reaction enthalpy for those reactions are typically in the range from 80 to 180 kJ mol^{-1}.

As in the case of sorption processes, the main drawbacks in solid–gas chemical reactions are the poor heat and mass transfer performance in the reactive bed and the low thermodynamic efficiency of the basic cycle (reactor temperature swing), which is critical for continuous operation. So far, the main research direction on chemical reaction heat pumps has been focused on improving the performance of the system by improving the design of the reactor and heat exchanger and by using composite materials.

3.2. Specific Reactants

3.2.1. Hydroxides

Kato et al. [126] developed a chemical heat pump based on the hydration and dehydration of $MgO/Mg(OH)_2$. The chemical heat pump is intended to recover waste heat from the exhaust gas of

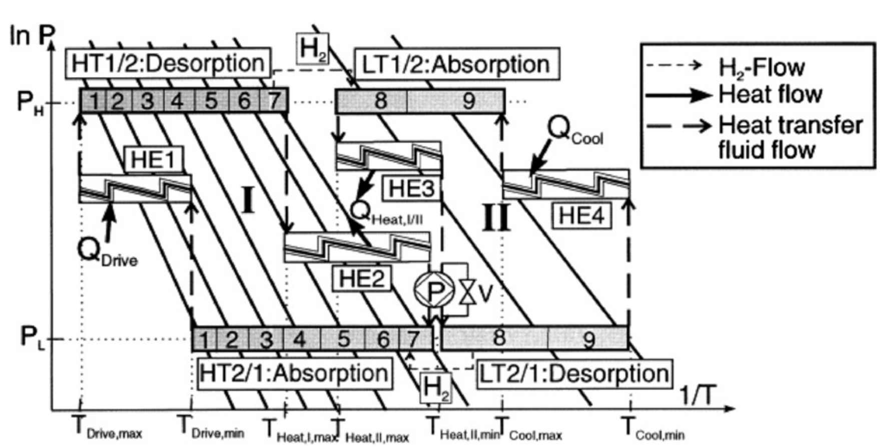


Fig. 13. Multi-hydride thermal wave scheme on the van Hoff diagram [124].

combustion engines (gas and diesel, such as cogeneration systems, vehicles, fuel cells, micro-gas turbines, etc.) at around 250–400 °C and to produce heat at around 100–250 °C with a water vapor pressure lower than 400 kPa [127]. The reactants used in the experiments were MgO made from ultra-fine particles with high purity and purified water because studies [128–130] showed that MgO had enough reactivity and high durability to repetitive reaction cycle. Kato et al. [131] obtained a mean heating power of 119 W kg_{salt}^{-1} during the initial 60 min, when the operating temperatures were 400 °C/30–200 °C/121 °C. In a later study [127], a carbon fiber sheet fin was used for thermal conductivity enhancement in the packed bed. The reported mean heating power was 49 W kg_{salt}^{-1} at temperatures of 150–160 °C during the initial 100 min, when the initial bed temperature was 120 °C, the evaporator temperature was 85 °C and the $Mg(OH)_2$ was previously dehydrated at 430 °C. Kato et al. [132] and Ryu et al. [133] also showed that when the $Mg(OH)_2$ was mixed with $Ni(OH)_2$ or $Co(OH)_2$ at atomic level, the new material was able to store heat at lower temperatures (200–300 °C), at which pure $Mg(OH)_2$ could not be dehydrated. Further research was carried out by Kim et al. [134] on the composite material made of expanded graphite and magnesium hydroxide to enhance the thermal conductivity and reactivity of magnesium oxide/water chemical heat pump. In addition, calcium chloride was also introduced into the mixture of expanded graphite and $Mg(OH)_2$ to ensure smooth diffusion of vapor in materials and enhance fit ability between expanded graphite and $Mg(OH)_2$. The composite material showed a higher reactivity than pure $Mg(OH)_2$.

Ogura and Mujumdar [135] proposed a chemical heat pump dryer (CHPD) based on the hydration and dehydration of CaO/$Ca(OH)_2$. The proposed CHPD consists of two chemical heat pumps (CHP), both based on the same chemical reaction. The pumps produced hot air for the drying room by using the heat released from the reaction or from the condensation of water (Fig. 14). The two CHPs, 1 and 2, operate concurrently in the heat enhancement mode. In Fig. 14, CHP1 is in the heat storing step (charging, Th > 594 °C and Tm ≅ 150 °C), while CHP2 is in the heat releasing step (discharging, Tm = 360 °C and Tl = 20 °C). After every hour or so, the two heat pumps swap operating steps. Ogura et al. [137] experimentally evaluated the performance of the chemical heat pump for the hydration reaction, i.e. CHP2 in Fig. 14. The experiments were performed in a multi tray packed bed reactor and each tray had radial fins for heat transfer enhancement. At the evaporation temperature of 20 °C and initial air temperature of 27 °C, the outlet air temperature from the heat exchanger achieved a maximum temperature of 187 °C rapidly and then decreased gradually to 47 °C after 600 min. The reported average heating power was 2.86 kW (477 W · kg_{salt}^{-1}) for 30 min operation while 1.77 kW (295 W · kg_{salt}^{-1}) for 60 min operation. Further studies by Ogura et al. [136,138] were focused on the controllability of the output characteristics of the CHP. The experiments were carried out at different operating temperatures for the heat storing step (T_h = 550–770 °C and T_m = 77 °C) and for the heat releasing step (T_l = 5–20 °C). In the heat storing step, the authors found that heat at 77 °C can be generated in the condenser even when the dehydration temperature is as low as 550 °C (30 % conversion after 170 min). On the other hand, in the heat releasing step, the authors found that heat at above 127 °C can be generated in the reactor even when the evaporator temperature was at 5 °C. Finally, they concluded that the CHP can be controlled by operating temperature and pressure control of the chemical reactions.

Cerkvenik et al. [139] tested a refrigeration chemical heat pump based also on the reversible hydration of CaO. The system was also proposed as a topping cycle of a gas-driven cascading sorption cooling device [140]. CaO was combined with expanded graphite by a suspension method. The mixture was then dried and pressed into the desired form. To increase the mass transfer of the reactive block, three vapor channels were made in the graphite matrix. The average SCP was about 50 kWh when the cycle time was limited to 1000 s (70 % conversion) at the water vapor pressure of 0.75 kPa (typical value for refrigeration) and hydration temperature of 200 °C. Moreover, the effect of three vapor channels was compared with a study carried out by Depta [141] in which only one vapor channel was used. At the hydration temperature of 200 °C with a water vapor pressure of 1.5 kPa, the authors found that the cycle time with three vapor channels was about four times higher than with one vapor channel.

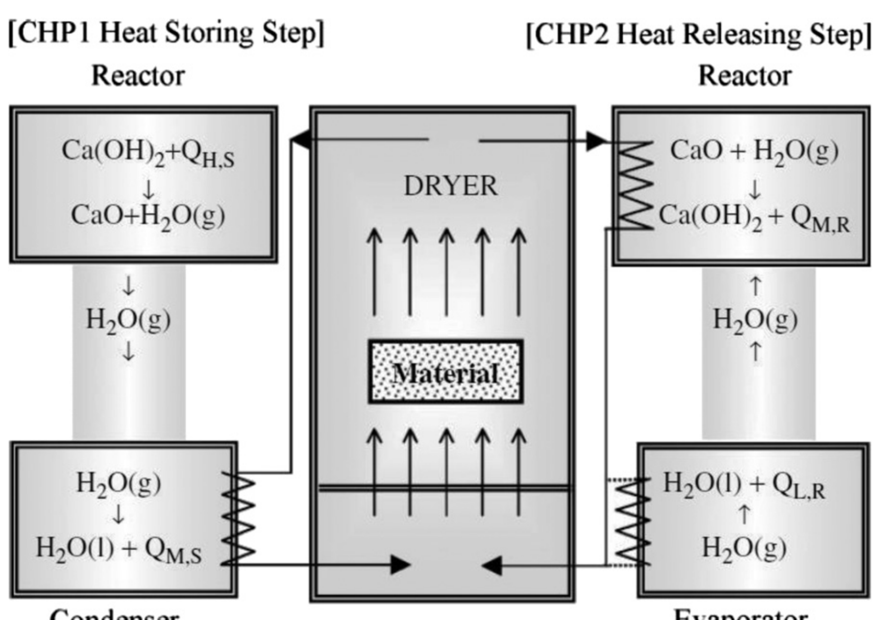


Fig. 14. Schematic diagram of the CaO/H_2O/$Ca(OH)_2$ CHPD system [135].

Table 1
Summary of the thermal performance of the chemical heat pumps based on sorption process between inorganic salts and ammonia over the last two decades.

Reagents	Additive	Mass (kg)	Th/ Tm/ Tc	SCP (w kg^{-1})	SHP(w kg^{-1})	Time (min)		COP (COPA)	Authors	Year	Application
						Half-cycle	cycle				
$BaCl_2$/ $MnCl_2$	EG (35 %)	3.27/ 3.96	195/ 50/ 25	300[b]	320	25	–	0.35	Lépinasse et al. [65]	1993	Refrigeration
$BaCl_2$/ $NiCl_2$	EG (35 %)	0.10/ 0.13	–/ −40/ 0	396[b]	–	15	–	–	Goetz et al. [69]	1996	Refrigeration
$SrCl_2$/ $CoCl_2$	EG (49 %/ 41%)	0.17/ 0.27[a]	240/ 7.5/ −4	145	–	–	–	0.25	Llobet and Goetz [76]	2000	Refrigeration
$MnCl_2$/ $NiCl_2$	EG	26.5/ 27[a]	280/ 10/ −5	29	–	–	–	0.21	Nevau et al. [77]	1992	Refrigeration
$SrBr_2$/ $NiCl_2$	EG	2.35/ 0.89[a]	340/ 8/ −4	134	–	–	–	0.38	Wagner [78]	1996	Refrigeration
$BaCl_2$	–	1	95–70/ 23/ 0−(−8)	–	–	90	–	–	Rivera et al. [99]	2007	Refrigeration
$BaCl_2$/ $MnCl_2$	EG (37 %)	0.23/ 0.27	180/ 30/ 10				140	0.64	Li et al. [60]	2009	Refrigeration
$BaCl_2$/ $MnCl_2$	EG (50 %)	–	180/ 30 25/ 10	301	–	60	–	0.62	Li et al. [67]	2009	Refrigeration
$BaCl_2$/ $MnCl_2$	EG (50 %)	–	180/ 30 25/ 10	–	–		150	0.64	Li et al. [68]	2010	Refrigeration
$CaCl_2$	AC (25 %)	2x1.88[a]	100/ 25/ −15	731	–		50	0.41	Wang et al. [81]	2006	Icemaker
$CaCl_2$	AC (25 %)	2x1.88[a]	113.7/ 30/ −19.4	528	–	–	70	0.26	Lu et al. [83]	2006	Icemaker
$CaCl_2$	AC (25 %)	2x1.88[a]	82.4/ 30/ −15.2	161			24	0.12	Lu et al. [83]	2006	Icemaker
$CaCl_2$	AC (25 %)	2x1.88[a]	126/ 27/ −7.5	325	–		36	0.2	Lu et al. [82]	2007	Icemaker
$CaCl_2$	AC (25 %)	7.4	160/ 10/ −18.9	486	–		20	0.27	Li et al. [84]	2007	Icemaker
$CaCl_2$	AC (25 %)	7.4	145/ 30/ −19.5	435	–		~36	0.25	Li et al. [85]	2008	Icemaker
$CaCl_2$	AC (25 %)	7.4	103/ 30/ −19.5	228	–		~27.5	0.14	Li et al. [85]	2008	Icemaker
$CaCl_2$	EG (50 %)	0.23	135/ 35 20/ −11	1500	–	–	–	0.35	Oliveira et al. [36]	2007	Icemaker
$CaCl_2$	EG (35 %)	–	97/ 30/ −18.3	255		40	–		Oliveira et al. [35]	2007	Icemaker
$CaCl_2$	EG (25 %)	2x33.75	110.6/ 25/ −15	303	–	–	25	0.32	Xia et al. [86]	2008	Refrigeration (icemaker)
LiCl	EG (50 %)	0.083	80/ 25/ −5	117[b]		30		0.47	Kiplagat et al. [100]	2009	Icemaker
$SrCl_2$	EG (35 %)	–	–	738	–	–	–	0.435	Chen et al. [101]	2010	Icemaker
$CaCl_2$	EG (25 %)	2x33.75	140/ 25/ −15	422	–		25	0.27	S.L. Li et al. [87]	2010	Refrigeration (icemaker)
$PbCl_2$/ $MnCl_2$	EG (35 %)	0.62/ 0.33	150/ 20/ 20	(47)[c]	–	120	–	–	Lépinasse et al. [70]	2001	Cooling a 88 L box
$BaCl_2$	EG (56 %)	38.1	–	–	–	–	1440	0.031	Le Pierres et al. [97]	2007	560 l cold box (−30 °C)
NH_4Cl/ $MnCl_2$	EG (20 %)	0.32/ 0.74	165/ AT/ AT	43/ 11–18	–	180	–	–	Bao et al. [72]	2011	Cooling and freezing a 33 L box
$MnCl_2$	EG (37 %)	–	180/ 25/ -30	350	–	30		0.34	Li et al. [37]	2009	Deep–freezing
NaBr	EG (50 %)	0.11	65/ 30/ 15	129[b]	–	40	–	0.46	Oliveira et al. [74]	2008	Air conditioning
NaBr/ $MnCl_2$	EG (35 %)	0.05/ 0.08	165/ 30 70/ 10	–	–	45		0.21 (1.11)	Oliveira et al. [74]	2008	Air conditioning
$BaCl_2$	EG	–	80/ 30/ 15	192	–	–	–	0.5	Chen et al. [98]	2009	Air conditioning
NH_4Cl/ $MnCl_2$	EG (33 %)	0.08/ 0.15	140/ 30 75/ 0	(1.12)[d]	(3.04)	360	720	0.35 (1.3)	Xu et al. [73]	2011	Heat & cold
$CoCl_2$	AC (30 %)	1.7	–	(235)[e]	–	–	–	–	Aidoun and Ternan [103]	2002	Heat & cold
$CaCl_2$	Busofit (70 %)	1.07	120/50/–18	–	–	–	25–30	0.43	Vasiliev et al. [91]	2001	Refrigeration
$BaCl_2$ + $NiCl_2$	Busofit (50 %/ 48 %)	0.55	240/50–/18	–	–	–	60	0.44	Vasiliev et al.[94]		Chilled water & steam
$BaCl_2$ + $MnCl_2$ + $NiCl_2$	Busofit	–	230 −180–90/–/–	–	–	–	–	0.41	Vasiliev et al. [94] Aristov and Vasiliev [95]	2003	Chilled water & steam
$BaCl_2$ + $MnCl_2$ + $NiCl_2$	Busofit	–	450–400–96/–/–	–	–	–	–	0.62	Vasiliev et al. [94] Aristov and Vasiliev [95]	2003	Chilled water & steam
$CaCl_2$/ $MnCl_2$	EG (50 %/ 40 %)	–	150/120/40	–	248	50		0.25	Wang et al. [75]	2010	Heat transformer
LiCl/ $MgCl_2$	Metal foam	1.8/ 1.8[a]	200/ 155 200/ 20	–	222	40	–	0.11	Haije et al. [39]	2007	Heat transformer
LiCl/ $MgCl_2$	Metal foam	1.2/ 2.49[a]	130/ 80 130/ 20	–	120	60	–	–	van der Pal et al. [42]	2009	Heat transformer
$CaCl_2$		3	–	–	–	–	–	1.2–2[f]	Fadhel et al. [88]	2010	Drying
$NiCl_2$	EG	–	300/ −200/–	–	–	–	–	0.17	Cerkvenik et al. [102]	2009	Topping cycle

Th is the heat source temperature (°C), Tm is the heat sink or condensing temperature (°C) and Tc is the cooling or evaporating temperature (°C). SCP is the average specific cooling power (W per kg of desorbing composite material) and SHP is the average specific heating power (w per kg of absorbing composite material).

[a] Mass of the anhydrous salt.
[b] w per kg of desorbing salt.
[c] kWh per m^3.
[d] $MJkg^{-1}day^{-1}$ (kg of absorbing composite).
[e] kW per m^3 (peak power).
[f] heating performance for the integrated chemical heat pump with solar collector and storage tank.

3.2.2. *Carbonates*

Kato et al. [142–145] also developed a double reactor type of heat transformer based on the reversible carbonation of calcium oxide (CaO) and lead (II) oxide (PbO) via carbon dioxide (CO_2). This chemical heat pump was developed to store heat in the CaO reactor from a high temperature process (e.g. $>860\,^{\circ}C$) and upgrade it to higher temperatures (e.g. $>900\,^{\circ}C$) for a gas turbine generator. In addition, the heat released during heat storing step from the carbonation of PbO could be used as the heat source of a steam-turbine. The authors obtained a mean heating power of $238\ W\ kg_{salt}^{-1}$ at temperatures of 925–990 °C during the initial 60 min of the heat releasing step, when the dehydration was carried out at 900 °C and 30.4 kPa (> 460 °C), and the hydration at 304 kPa with an initial bed temperature of 900 °C.

4. Conclusions

This paper presented a state-of-the-art review of the current experimental research on chemical sorption (chemisorption) process and chemical reactions based on solid–gas systems for thermal energy storage and conversion. Tables 1–4 give a summary of the experimental thermal performances under practical conditions obtained by the different prototypes built over the last two decades. These results are a merely indication of the efficiency and power of such systems and should not be compared as they are obtained under different working conditions.

Refrigeration technologies based on metal salts and ammonia has progressed considerably over the last twenty years. Consolidated composite materials have shown their potential to increase the cooling performance and currently, specific cooling powers over 700 W per kilogram of desorbing materials were reached by some ice making prototypes.

Recently, Linder et al. [122] also obtained a SCP as high as 780 $W\cdot kg^{-1}$ with a metal hydride air conditioner prototype that used a capillary bundle reactor to increase the heat transfer rate. However, generally, the SCP obtained with the experimental prototypes using metal hydrides is much lower than that obtained with salt ammoniates. Muthukumar and Groll [25] have also pointed out the use of composite materials and advanced cycles concepts as future research lines to increase the efficiency and reduce the cost of these systems.

By contrast, the reported experimental COP for the current prototypes is still low, usually raging from 0.2–0.65. According to Meunier [17] in order to reduce the contribution of a sorption system to the greenhouse effect with respect to compression system, the cooling COP should be at least equal to 1. Although, sorption heat pumps with a COP of less than 1 may be recommended if they use renewable energy sources.

The research on chemical sorption process and chemical reactions for heating applications was less than for cooling applications, and was mainly related to chemical reactions. However, in the past few years, new working pairs appeared for chemical sorption systems. The current research direction is also focused to demonstrate the feasibility of these technologies under practical conditions by improving the heat and mass transfer in the solid bed. So far the specific heating powers of the current system are in the range from 100 to 300 $W\ kg^{-1}$.

Therefore, the main research direction for future research can be summarized in the following points:

- Although researchers obtained promising experimental results with consolidated composite materials, improvements on heat transfer often results in a deployment of mass transfer [23,28]. In cases of low operating vapor pressures (water, methanol), the reactor requires of a short mass transfer path (thickness)

Table 2
Summary of the thermal performance of the chemical heat pumps based on sorption process between inorganic salts and water over the last two decades.

Material	Additive	Mass salt (kg)	Th/ Tm/ Tc	SCP[c] ($w\ kg^{-1}$)	SHP ($w\ kg^{-1}$)	Time (min)		COP (COA)	Author	Year	Application
						Half–cycle	cycle				
$MgSO_4$	–	0.04	150/10 50/10	–	–	–	–	–	van Essen et al. [6]	2009	Seasonal heat storage
$Al_2(SO_4)$	–	0.04	150/10 50/10	–	–	–	–	–	van Essen et al. [106]	2009	Seasonal heat storage
$CaCl_2$	–	0.04	150/10 50/10	–	–	–	–	–	van Essen et al. [106]	2009	Seasonal heat storage
$MgCl_2$	Cellulose	3.6(2)	135/10 25/10	–	–	–	–	–	Zondag et al. [107]	2010	Seasonal heat storage
Na_2S	Cellulose	3	86–77/25–15 –/20–5	500[a]	–	–	–	0.57	De Boer et al. [109]	2004	Heating & cooling
$SrBr_2$	EG (6 %)	0.14	70/35/12		26[b]	~376	–	–	Lahmidi et al. [111]	2006	Heating (winter) & cooling (summer)
$SrBr_2$	EG (6 %)	0.14	70/35/12	49[b]		~188	–	–	Lahmidi et al. [111]	2006	Heating (winter) & cooling (summer)
$SrBr_2$	EG (8 %)	171.3	70/12 35/12	–	13	–	–	–	Mauran et al. [112]	2008	Heating (winter) & cooling (summer)
$SrBr_2$	EG (8 %)	171.3	70/35/18	15	–	840	–	–	Mauran et al. [112]	2008	Heating (winter) & cooling (summer)
$MnCl_2$	EG (20 %)	4.56	330–320/120–145 145–160/95	–	–	–	87	(1.25)	Stitou et al. [110]	2004	Heat transformer

Th is the heat source temperature (°C), Tm is the heat sink or condensing temperature (°C) and Tc is the cooling or evaporating temperature (°C). SCP is the average specific cooling power (W per kg of desorbing composite material) and SHP is the average specific heating power (w per kg of absorbing composite material).

[a] highest specific cooling power (w per kg of Na_2S).
[b] kw per m^3.

Table 3
Summary of the thermal performance of the metal hydride heat pumps over the last two decades.

Metal hydrides	Mass (kg)	Th/ Tm/ Tc	SCP ($w\ kg^{-1}$)		SHP ($w\ kg^{-1}$)	Time (min)		COP (COA)	Authors	Year
			Cooling cycle	Whole cycle		Cycle	Half–cycle			
$Zr_{0.9}$ $Ti_{0.1}Cr_{0.6}Fe_{1.4}$/ $Zr_{0.9}Ti_{0.1}Cr_{0.9}Fe_{1.1}$	2.5/2	200/30/18	–	151	–	–	12–	–	Lee et al. [113]	1996
$LaNi_{4.6}Mn_{0.3}Al_{0.1}$/ $La_{0.6}Y_{0.4}Ni_{4.8}Mn_{0.2}$	90	140/ 20/ −15	80[a]	41	–	–	−19	0.42	Imoto et al. [114]	1995
$MmNi_{4.5}Al_{0.5}$/ ZrMnFe	0.8/ 0.7	130–110/ 25–30/ 5–15	60–90	30–45	–	3–12	–	0.2–0.35	Gopal and Murthy [115]	1999
Thermal wave	–	235/ 33/ 18	20[a]	10[a]	–	–	25	0.33	Willers et al. [41]	1999
$LaNi_{4.7}Al_{0.3}$/ $MmNi_{4.15}Fe_{0.85}$	4.5/ 5.7	140/ 30/ 20	–	–	–	10	20	0.2	Kang et al. [117]	1996
$LmNi_{4.85}Sn_{0.15}$/ $LmNi_{4.49}Co_{0.1}Mn_{0.205}Al_{0.205}$/ $LmNi_{4.08}Co_{0.2}Mn_{0.62}Al_{0.1}$	70/ 70/ 70	190/ 130/ 40	–	–	–	10	20	–	Willer and Groll [118]	1999
$MmNi_{4.15}Fe_{0.85}$/ $LaNi_{4.6}Al_{0.4}$	1.5/ 1.5[a]	130/ 25/ 1.5[a]	–	100[a]	–	20	–	0.33	Chernikov et al. [116]	2002
$LaNi_{4.1}Al_{0.52}Mn_{0.38}$/ $LmNi_{4.91}Sn_{0.15}$/ $Ti_{0.99}Zr_{0.01}V_{0.43}Fe_{0.09}Cr_{0.05}Mn_{1.5}$	15.7/ 14.8/ 14.4	330/ 100 23/ 16–2	–	–	–	–	–	0.51 (0.86)	Klein et al. [40]	2007
$La_{0.6}Y_{0.4}Ni_{4.8}Mn_{0.2}$/ $LaNi_{4.61}Mn_{0.26}Al_{0.13}$	5.5/ 5.5	150/ 30/ 0	–	15.4	–	–	60	0.26	Qin et al. [120]	2007
$La_{0.6}Y_{0.4}Ni_{4.8}Mn_{0.2}$/ $LaNi_{4.61}Mn_{0.26}Al_{0.13}$	5.5/5.5	130/30 32/20	–	44.4	–	–	64	0.3	Ni and Liu [121]	2007
$Ti_{0.99}Zr_{0.01}V_{0.43}Fe_{0.09}Cr_{0.05}Mn_{1.5}$/ $LmNi_{4.91}Sn_{0.15}$	0.9/ 0.9	130/ 28/ 20	780	–	–	2.15	–	–	Linder et al. [122]	2010

Th is the heat source temperature (°C), Tm is the heat sink temperature (°C) and Tc is the cooling temperature (°C). SCP is the average specific cooling power (W per kg of desorbing material).

[a] According to Muthukumar et al. [25].

Table 4
Summary of the thermal performance of the chemical heat pumps based on solid–gas chemical reactions over the last two decades.

Reagents	Additive	Mass (kg)	Th/ Tm/ Tc	SCP ($w\ kg^{-1}$)	SHP ($w\ kg^{-1}$)	Time		COP (COPA)	Author	Year	Application
						Half–cycle	Cycle				
$Mg(OH)_2/MgO$	–	0.052	400/30 145/121	–	119	60	–	–	Kato et al. [131]	2005	Heat amplifier
$Ca(OH)_2/CaO$	–	–	>594/150 360/20	–	295	60	–	–	Ogura et al. [137]	2001	Drier
$Ca(OH)_2/CaO$	EG (50%)	0.0187	440/3 200/3	225	–	17	–	–	Cerkvenik et al. [139]	2002	Refrigeration
$CaCO_3/CaO + PbCO_3/PbO$	–	1/–	900/300 900/460	–	225[b]	60	–	–	Kato et al. [145]	2001	Turbine

Th is the heat source temperature (°C), Tm is the heat sink or condensing temperature (°C) and Tc is the cooling or evaporating temperature (°C). SCP is the average specific cooling power (W per kg of material) and SHP is the average specific heating power (W per kg of material).

[b] Calculated from experiments.

and large number of mass transfer channels which reduces power output per volume of reactor [26,28,46].Therefore, research efforts are needed towards developing advanced composite materials with good heat and mass transfer and development of advanced designs and configuration for reactor and heat exchanger.

- Testing and developing advanced cycles designs to improve the COP, towards 1 or further. In addition, cascading cycles can be used to improve the efficiency of the current commercial absorption devices. The chemical sorption or reaction heat pump is used as the topping cycle as it can be driven at higher temperature than the absorption devices.
- Perform long-duration test to study the durability and stability of the material. According to Wang et al. [48] problems of expansion, decomposition, deterioration and corrosion in the chlorides salts-ammonia systems are the main drawback for its widespread utilization.
- Built and test larger scale prototypes (more modules or larger reactors) to prove the same SCP or SHP and COP as with the current prototypes (small-scale).
- Intensification of the experimental research on chemical sorption process and chemical reaction systems for heating applications as the scope for its application is very wide, especially for chemical reactions. The potential of chemical reaction heat pump systems lies on the fact that they work at very high temperatures which no other commercial heat pump can reach.
- Although, the research for short or long term thermal storage is in the early stage, only few experiments have been carried out for short discharging periods. More experiments are required to demonstrate the feasibility for short and long term heat storage.
- Finally, another important point for its application is that these technologies are operated under a variable waste heat temperature. Therefore, a control strategy of these systems should be optimized in order to obtain a high efficiency [20].

Although much more research efforts are needed to bring these technologies to the market, the advanced technology development have been reflected on the experimental results.

Acknowledgments

The work is partially funded by the Spanish government (ENE2008-06687-C02-01/CON and ENE2011-22722). The authors would like to thank the Catalan Government for the quality accreditation given to their research group GREA (2009 SGR 534).

References

[1] IEA. Renewables for heating and cooling: untapped potential—a joint report for the renewable energy technology deployment implementing agreement and the renewable energy working party of the International Energy Agency. International Energy Agency. 〈http://www.iea.org〉; 2007 [accessed 15.10.11].
[2] Arce P, Medrano M, Gil A, Oró E, Cabeza LF. Overview of thermal energy storage (TES) potential energy savings and climate change mitigation in Spain and Europe. Applied Energy 2011;88:2764–74.
[3] IEA. Co-generation and Renewables. Solutions for a low-carbon energy future. International Energy Agency. 〈http://www.iea.org〉; 2011 [accessed 15.10.2011].
[4] Ma Q, Luo L, Wang RZ, Sauce G. A review on transportation of heat energy over long distance: Exploratory development. Renewable and Sustainable Energy Reviews 2009;13:1532–40.
[5] Kato Y. Thermal energy storages in Vehicles for fuel efficiency improvement. In: Proceedings of the 11th International Conference on Thermal Energy Storage—Effstock 2009 Stockholm, Sweden; 2009.
[6] van Essen VM, Zondag HA, Cot Gores J, Bleijendaal LPJ, Bakker M, Schuitema R, et al. Characterization of $MgSO_4$ hydrate for thermochemical seasonal heat storage. Journal of Solar Energy Engineering, Transactions of the ASM 2009;131(3):0410141–7.
[7] Hadorn J-C. Thermal energy storage for solar and low energy building. State of the art. IEA Solar Heating and Cooling Task 32: International Energy Agency; 2005.
[8] Gil A, Medrano M, Martorell I, Lázaro A, Dolado P, Zalba B, et al. State of the art on high temperature thermal energy storage for power generation. Part 1-Concepts, materials and modellization. Renewable and Sustainable Energy Reviews 2010;14:31–5.
[9] Medrano M, Gil A, Martorell I, Potau X, Cabeza LF. State of the art on high temperature thermal energy storage for power generation. Part 2-Case studies. Renewable and Sustainable Energy Reviews 2010;14:56–72.
[10] Paksoy HÖ. Thermal energy storage for sustainable energy consumption. fundamentals, Case Studies and Design: Springer in cooperation with NATO Public Diplomacy Division; 2007.
[11] Dinçer I, Rosen MA. Thermal energy storage. systems and applications. London: Wiley; 2002.
[12] Mehling H, Cabeza LF. Heat and cold storage with PCM. An up to date introduction into basics and applications. Berlin Heidelberg: Springer-Verlag; 2008 Berlin.
[13] Nevau P, Castaing J. Solid–gas chemical heat pumps: fields of application and performance of the internal heat of reaction recovery process. Heat Recovery Systems & CHP 1993;13(3):233–51.
[14] Goetz V, Elie F, Spinner B. The structure and performance of single effect solid/gas chemical heat pumps. Heat Recovery Systems & CHP 1993;13(1):79–96.
[15] Li TX, Wang RZ, Oliveira RG, Wang LW. Performance analysis of an innovative multimode, multisalt and multieffect chemisorption refrigeration system. AIChE Journal 2007;53(12):3222–30.
[16] Li TX, Wang RZ, Kiplagat JK, Chen H, Wang LW. A new target-oriented methodology of decreasing the regeneration temperature of solid–gas thermochemical sorption refrigeration system driven by low-grade thermal energy. International Journal of Heat and Mass Transfer 2011;54:4719–29.
[17] Meunier F. Solid Sorption: an alternative to CFCs. Heat Recovery Systems and CHP 1993;13(4):289–95.
[18] Ervin G. Solar heat storage using chemical reactions. Journal of solid state chemistry 1977;22:51–61.
[19] Yu YQ, Zhang P, Wu JY, Wang RZ. Energy upgrading by solid–gas reaction heat transformer: a critical review. Renewable and Sustainable Energy Reviews 2008;12:1302–24.
[20] Deng J, Wang RZ, Han GY. A review of thermally activated cooling technologies for combined cooling, heating and power systems. Progress in Energy and Combustion Science 2011;37:172–203.
[21] Hauer A. Thermal energy storage for sustainable energy consumption. sorption theory for thermal energy storage. Netherlands: Springer; 2007 pp 393-408.
[22] Han JH. K-H. L. Effective thermal conductivity of graphite-metallic SALT complex for Chemicals heat pumps. Journal of Thermophysics and Heat Transfer 1999;13:481–8.
[23] Mauran S, Prades P, L'Haridon F. Heat and mass transfer in consolidated reacting beds for thermochemical systems. Heat Recovery Systems and CHP 1993;13(4):315–9.
[24] Wang K, Wu JY, Wang RZ, Wang LW. Effective thermal conductivity of expanded graphite-$CaCl_2$ composite adsorbent for chemical adsorption chillers. Energy Conversion and Management 2006;47:1902–12.
[25] Muthukumar P, Groll M. Erratum to Metal hydride based heating and cooling systems: a review. International Journal of Hydrogen Energy 2010;35:8816–29.
[26] Meunier F. Solid sorption heat powered cycles for cooling and heat pumping applications. Applied Thermal Engineering 1998;18:715–29.
[27] Abhat A, Huy TQ. Heat and mass transfer considerations in a thermochemical energy storage system based on solid–gas reactions. Solar Energy 1983;32(2):93–8.
[28] Han JH, Lee K-H. Gas permeability of expanded graphite-metallic salts composite. Applied Thermal Engineering 2001;21:453–63.
[29] Dellero T, Sarmeo D. Ph. T. A chemical heat pump using carbon fibers as additive. Part I: enhancement of thermal conduction. Applied Thermal Engineering 1999;19:991–1000.
[30] Meunier F, Kaushik SC, Neveu P, Poyelle F. A comparative thermodynamic study of sorption systems: second law analysis. International Journal of Refrigeration 1996;19(6):414–21.
[31] Coste C, Crozat G, Mauran S. Societe Nationale Elf Aquitaine, assignee. Gaseous-Solid Reaction US Patent 4,595,774; 1986.
[32] Zhang P, Wang C, Wang R. Composite reactive block for heat transformer system and improvement of system performance. International Journal of Chemical Engineering of Japan 2007;40(13):1275–80.
[33] Bou P, Moreau M, Prades P. Elf Aquitaine and Le Carbone Lorraine, assignee. Active composites with foliated structure and its use as reaction medium US Patent 5,861,207; 1999.
[34] Mauran S, Lebrun M, Prades P, Moreau M, Spinner B, Drapier C. Societe Nationale Elf Aquitaine and Le Carbone Lorraine, assignee. Active composite and its use as reaction medium US Patent 5,283,219; 1994.
[35] Oliveira RG, Wang RZ. A consolidated calcium chloride-expanded graphite compound for use in sorption refrigeration systems. Carbon 2007;45:390–6.
[36] Oliveira RG, Wang RZ, Wang C. Evaluation of the cooling performance of a consolidated expanded graphite-calcium chloride reactive bed for chemisorption icemaker. International Journal of Refrigeration 2007;30:103–12.

[37] Li TX, Wang RZ, Kiplagat JK, Wang LW. Performance study of a consolidated manganese chloride-expanded graphite compound for sorption deep-freezing processes. Applied Energy 2009;86:1201–9.
[38] Wank K, Wu YU, Wang RZ, Wang LW. Composite adsorbent of $CaCl_2$ and expanded graphite for adsorption ice maker on fishing boats. International Journal of Refrigeration 2006;29:199–210.
[39] Haije WG, Veldhuis JBJ, Smeding SF, Grisel RJH. Solid/vapour sorption heat transformer: design and performance. Applied Thermal Engineering 2007;7: 1371–6.
[40] Klein H-P Betriebsverhalten einer zweistufigen Metallhydrid-Sorptionsanlage zur Kälteerzeugung: Universität Stuttgart; 2007. [In German].
[41] Willers E, Wanner M, Groll M. A Multi-hydride thermal wave device for simulations heating and cooling. Journa of Alloys and Compounds 1999;293-295:915–8.
[42] van der Paal M, de Boer R, Veldhuis JBJ, Smeding SF 2009. Thermally driven ammonia-salt type II heat pump: development and test of a prototype. Energy Research Centre of the Netherlands (ECN). Report nr ECN-M—09-059 last.
[43] Aidoun Z, Ternan M. Salt impregnated carbon fibres as the reactive medium in a chemical heat pump: the NH_3–$CoCl_2$ system. Applied Thermal Engineering 2002;22:1163–74.
[44] Vasiliev LL, Kanonchik LE, Antuh AA, Kulakov AG. NaX Zeolite, Carbon Fibre and $CaCl_2$ ammonia reactors for heat pumps and refrigerators. Adsorption 1996;2:311–6.
[45] Wang LW, Wang RZ, Wu JY, Wang K. Compound adsorbent for adsorption ice maker on fishing boats. International Journal of Refrigeration 2004;27:401–8.
[46] Wang LW, Wang RZ, Oliveira RG. A review on adsorption working pairs for refrigeration. Renewable and Sustainable Energy Reviews 2009;13:518–34.
[47] Wang RZ, Oliveira RG. Adsorption refrigeration—An efficient way to make good use of waste heat and solar energy. Progress in Energy and Combustion Science 2006;32:424–58.
[48] Wang DC, Li YH, Li D, Xia YZ, Zhang JP. A review on adsorption refrigeration technology and adsorption deterioration in physical adsorption systems. Renewable and Sustainable Energy Reviews 2010;14:344–53.
[49] Shelton SV. Solid adsorbent heat pump system US Patent 4,610,148; 1986.
[50] Tchernev DI. Heat pump energized by low-grade heat source US Patent 4,637,218; 1987.
[51] Shelton SV, Wepfer WJ, Miles DJ. Ramp wave analysis of the solid/vapor heat pump. Journal of Energy Resources Technology 1990;112(1):69–78.
[52] Critoph RE. Forced convection enhancement of adsorption cycles. Heat Recovery Systems and CHP 1994;14(4):343–50.
[53] Critoph RE. Forced convection adsorption cycles. Applied Thermal Engineering 1998;18(9-10):799–807.
[54] Meunier F. Theoretical performances of solid adsorbent cascading cycles using the zeolite-water and active carbon-methanol pairs: four case studies. Journal of Heat Recovery Systems 1986;6(6):491–8.
[55] Douss N, Meunier FE, Sun LM. Predictive model and experimental results for a two-adsorber solid adsorption heat pump. Industrial & Engineering Chemistry Research 1988;27(2):310–6.
[56] Pons M, Poyelle F. Adsorptive machines with advanced cycles for heat pumping or cooling applications: cycles a adsorption pour pompes a chaleur ou machines frigor: figues. International Journal of Refrigeration 1999;22(1):27–37.
[57] Wang RZ. Performance improvement of adsorption cooling by heat and mass recovery operation. International Journal of Refrigeration 2001;24: 602–11.
[58] Spinner B. Ammonia-based thermochemical transformers. Heat Recovery Systems and CHP 1993;13(4):301–7.
[59] Vasiliev LL, Kulakov AG. Heat pipe applications in sorption refrigerators. Low temperature and cryogenic refrigeration. Netherlands: Springer; 2003 pp 401-414.
[60] Li TX, Wang RZ, Oliveira RG, Kiplagat JK, Wang LW. A combined double-way chemisorption refrigeration cycle based on adsorption and resorption processes. International Journal of Refrigeration 2009;32:47–57.
[61] Saha BB, Boelman EC, Kashiwagi T. Computational analysis of an advanced adsorption-refrigeration cycle. Energy 1995;20(10):983–94.
[62] Saha BB, Akisawa A, Kashiwagi T. Solar/waste heat driven two-stage adsorption chiller: the prototype. Renewable Energy 2001;23(1):93–101.
[63] Saha BB, Koyama S, Kashiwagi T, Akisawa A, Ng KC, Chua HT. Waste heat driven dual-mode, multi-stage, multi-bed regenerative adsorption system. International Journal of Refrigeration 2003;26(7):749–57.
[64] Lépinasse E, Spinner B. Production de froid par couplage de réacteurs solide-gaz I: analyse des performances de tels systèmes. Revue International du Froid 1994;17(5):309–22 [In French].
[65] Lépinasse E, Spinner B. Production de froid par couplage de réacteurs solide-gaz II: performance d'un pilote de 1 à 2 kW. Rev Int Froid 1994;17(5):323–8 [In French].
[66] Lépinasse E, Goetz V, Crozat G. Modelling and experimental investigation of a new type of thermochemical transformer based on the coupling of two solid–gas reactions. Chemical Engineering and Processing 1994;33:125–34.
[67] Li TX, Wang RZ, Kiplagat JK, Wang LW, Oliveira RG. Thermodynamic study of a combined double-way solid–gas thermochemical sorption refrigeration cycle. International Journal of Refrigeration 2009;32:1570–8.
[68] Li TX, Wang RZ, Chen H, Wang LW, Kiplagat JK. Performance improvement of a combined double-way thermochemical sorption refrigeration cycle with reheating process. AIChE Journal 2010;56(2):477–84.
[69] Goetz V, Spinner B, Lepinasse E. A solid–gas thermochemical cooling system using $BaCl_2$ and $NiCl_2$. Energy 1997;22(1):49–58.
[70] Lépinasse E, Marion M, Goetz V. Cooling storage with a resorption process. Application to a box temperature control. Applied Thermal Engineering 2001;21:1251–63.
[71] Bao HS, Oliveira RG, Wang RZ, Wang LW. Choice of low temperature salt for a resorption refrigerator. Industrial & Engineering Chemistry Research 2010;49:4897–903.
[72] Bao HS, Wang RZ, Wang LW. A resorption refrigerator driven by low grade thermal energy. Energy Conversion and Management 2011;52:2339–44.
[73] Xu J, Oliveira RG, Wang RZ. Resorption system with simultaneous heat and cold production. International Journal of Refrigeration 2011;34:1262–7.
[74] Oliveira RG, Wang RZ, Kliplagat JK, Wang CY. Novel composite sorbent for resorption systems and for chemisorption air conditioners driven by low generation temperature. Renewable Energy 2009;34:2757–64.
[75] Wang C, Zhang P, Wang RZ. Performance of solid–gas reaction heat transformer system with gas valve control. Chemical Engineering Science 2010;65:2910–20.
[76] Llobet J, Goetz V. Production de froid par transformation thermochimique: expérimentation d'un nouveau système à double effet à contact. International Journal of Refrigeration 2000;23:312–29 [In French].
[77] Nevau P, Castaing J, Mazet N, Meyer P. Performances expérimentales de thermotransformateurs hautes températures et machines à froid à double effet à base d'ammoniacates. In: Proceedings of the Symposium Le froid à sorption solide Paris, France; 1992. pp 173–178. [In French].
[78] Wagner A. Systèmes thermochimiques à soprtion solid–gaz à multiples effets, gérés par caloducs: Université de Perpignan; 1996. [in French].
[79] van der Paal M, de Boer R, Veldhuis JBJ, Smeding SF 2011. Experimental setup for determining ammonia-salt adsorption and desorption behaviour under typical heat pump conditions: a description of the setup and experimental results. Energy Research Centre of the Netherlands (ECN). Report nr ECN-M—11-030 last.
[80] van der Paal M, Veldhuis JBJ 2010. Thermodynamic properties of lithium chloride ammonia complexes under heat pump type II working conditions. Energy Research Centre of the Netherlands (ECN). Report nr ECN-M—10-076 last.
[81] Wang LW, Wang RZ, Lu ZS, Xu YX, JY WU. Split heat pipe type compound adsorption ice making test unit for fishing boats. International Journal of Refrigeration 2006;29:456–68.
[82] Lu ZS, Wang RZ, Li TX, Wang LW, Chen CJ. Experimental investigation of a novel multifunction heat pipe solid sorption icemaker for fishing boats using $CaCl_2$/activated carbon compound-ammonia. International Journal of Refrigeration 2007;30:76–85.
[83] Lu ZS, Wang RZ, Wang LW, Chen CJ. Performance analysis of an adsorption refrigerator using activated carbon in a compound adsorbent. Carbon 2006;44:747–52.
[84] Li TX, Wang RZ, Wang LW, Lu ZS, Chen CJ. Performance study of a high efficient multifunction heat pipe type adsorption ice making system with novel mass and heat recovery processes. International Journal of Journal of Thermal Sciences 2007;46:1267–74.
[85] Li TX, Wang RZ, Wang LW, Lu ZS. Experimental investigation of an innovative dual-mode chemisorption refrigeration system based on multifunction heat pipes. International Journal of Refrigeration 2008;31:1104–12.
[86] Xia ZZ, Li SL, Wu JY, Li J, Wang RZ. Experiment investigation of a novel adsorption deep freezing system using a new type of composite adsorbent. In: Proceedings of International Sorption Heat Pump Conference Hoam Convention Center, Seoul National University; 2008.
[87] Li SL, Xia ZZ, Wu JY, Li J, Wang RZ, Wang LW. Experimental study of a novel $CaCl_2$/expanded graphite-NH_3 adsorption refrigerator. International Journal of Refrigeration 2010;33:61–9.
[88] Fadhel MI, Sopian K, Daud WRW. Performance analysis of solar-assisted chemical heat-pump dryer. Solar Energy 2010;84:1920–8.
[89] Ibrahim M, Sopian K, Daud WRW, Alghoul MA. An experimental analysis of solar-assisted chemical heat pump dryer. International Journal of Low-Carbon Technology 2009;4(2):78–83.
[90] Ibrahim M, Daud WRW, Ibrahim K, Zaharim A, Sopian K. Performance of solid–gas chemical heat pump subsytem of solar dryer. In: Proceedings of American conference on Applied mathematics (AMERICAN-MATH'10) Cambridge, USA; 2010.
[91] Vasiliev LL, Mishkinis DA, Antukh AA, Vasiliev LL. Solar-gas solid sorption refrigerator. Adsorption 2001;7:149–61.
[92] Vasiliev LL, Mishkinis DA, Antukh AA, Vasiliev LL. Resorption heat pump. Applied Thermal Engineering 2004;24:1893–903.
[93] Vasiliev LL, Mishkinis DA, Antukh AA, Kulakov AG, Vasiliev LL. Multisalt-carbon portable resorption heat pump. In: Kakaç S, Smirnov HF, Avelino MR, editors. Low Temperature and Cryogenic Refrigeration. Kluwer Academic Publishers; 2003. p. 387–400.
[94] Vasiliev LL, Filatova OS, Tsitovich AP. Application of sorption heat pumps for increasing of new power sources efficiency. Archive of Thermodynamics 2010;31(2):21–4.
[95] Aristov IY, Vasiliev LL. New composite sorbents of water and ammonia for chemical and adsorption heat pump. Journal of Engineering Physics and Thermophysics 2006;79(6):1214–23.

[96] Le Pierrès N, Stitou D, Mazet N. New deep-freezing process using renewable low-grade heat: from the conceptual design to experimental results. Energy 2007;32:600–8.
[97] Le Pierrès N, Mazet N, Stitou D. Experimental results of a solar powered cooling system at low temperature. International Journal of Refrigeration 2007;30:1050–8.
[98] Chen H, Li T, Wang L, Wang R, Oliveira RG. Sorption performance of consolidated composite sorbent used in solar-powered sorption air-conditioning system. Huagong Xuebao/CIESC Journal 2009;60(5):1097–103 [In Chinese].
[99] Rivera C, Pilatowsky I, Méndez E, Rivera W. Experimental study of a thermo-chemical refrigerator using barium chloride-ammonia reaction. International Journal of Hydrogen Energy 2007;32:3154–8.
[100] Kiplagat JK, Wang RZ, Oliveira RG, Li TX. Lithium chloride—Expanded graphite composite sorbent for solar powered ice maker. Solar Energy 2010;84:1587–94.
[101] Chen H, Wu J-Y, Li TX, Wang RZ. Strontium chloride-expanded graphite consolidated composite adsorbent used in ice-making systems. Kung Cheng Je Wu Li Hsueh Pao/Journal of Engineering Thermophysics 2010;31(4): 561–4 [In Chinese].
[102] Cerkvenik B, Stitou D, Storkenmaier F, Ziegler F Measurement results for the novel NH_3–$NiCl_2(NH_3)2/6$ reaction cooling device. In: Proceedings of 2nd International Heat Powered Cycles Conference Paris, France; 2001.
[103] Aidoun Z, Ternan M. The synthesis reaction in a chemical heat pump reactor filled with chloride impregnated carbon fibres: the NH_3-$CoCl_2$ system. Applied Thermal Engineering 2002;22:1943–54.
[104] Trudel J, Hossatte S, Ternan M. Solid–gas equilibrium in chemical heat pumps: the NH_3–$CoCl_2$ system. Applied Thermal Engineering 1999;19: 495–511.
[105] Aidoun Z, Ternan M. Pseudo-stable transitions and instability in chemical heat pumps: the NH_3–$CoCl_2$ system. Applied Thermal Engineering 2001;21: 1019–34.
[106] van Essen VM, Cot Gores J, Bleijendaal LPJ, Zondag HA, Schuitema R, Bakker M, et al.. Characterization of salt hydrates for compact seasonal thermochemical storage. In: Proceedings of Proceedings of the ASME 3rd International Conference on Energy Sustainability 2009 San Francisco, USA; 2009. pp 825–830.
[107] Zondag HA, van Essen VM, Bleijendaal LPJ, Kikkert BWJ, Bakker M Application of MgCl2.6H2O for thermochemical seasonal solar heat storage. In: Proc Presented at 5th International Renewable Energy Storage Conference IRES 2010 Berlin, Germany; 2010.
[108] Zondag HA, Essen VMv, Bleijendaal LPJ, Kikkert BWJ, Bakker M Economical feasibility of sorption heat storage. In: Proceedings of the 5th International Renewable Energy Storage Conference IRES 2010 Berlin, Germany; 2010.
[109] De Boer R, Haije WG, Veldhuis JBJ, Smeding SF. Solid-sorption cooling with integrated thermal storage: The SWEAT prototype. Energy Research Centre of the Netherlands (ECN). Report nr ECN-RX—04-080. Last; 2004.
[110] Stitou D, Mazet N, Bonnissel M. Performance of a high temperature hydrate solid/gas sorption heat pump used as topping cycle for cascaded sorption chillers. Energy 2004;29:267–85.
[111] Lahmidi H, Mauran S, Goetz V. Definition, tests and simulation of a thermochemical storage process adapted to solar thermal system. Solar Energy 2009;80:883–93.
[112] Mauran S, Lahmidi H, Goetz V. Solar heating and cooling by a thermochemical process. First experiments of a prototype storing 60 kWh by a solid/gas reaction. Solar Energy 2008;82:623–36.
[113] Lee SG, Kim KY, Lee JY. Operating characteristics of metal hydride heat pump using Zr-based laves phases. International Journal of Hydrogen Energy 1995;20(1):77–85.
[114] Imoto T, Yonesaki T, Fujitani S, Yonezy I, Hiro N, Nasako K. Development of an F-class refrigeration system using hydrogen-absorbing allows. International Journal of Hydrogen Energy 1996;21(6):451–5.
[115] Gopal MR, Murthy SS. Experiments on a metal hydride cooling system working with ZrMnFe/MmNi4.5Al0.5 pair. International Journal of Refrigeration 1999;22:137–49.
[116] Chernikov AS, Izhvanov LA, Solovey AI, Frolov VP, Shanin YI. An installation for water cooling based on a metal hydride heat pump. Journal of Alloys and Compounds 2002;330-330:907–10.
[117] Kang BH, Park CW, Lee CS. Dynamic behaviour of heat and hydrogen transfer in a metal hydride cooling system. International Journal of Hydrogen Energy 1996;21(9):769–74.
[118] Willers E, Groll M. The two-stage metal hydride heat transformer. International Journal of Hydrogen Energy 1999;24:269–76.
[119] Klein H-P, Groll M. Development of a two-stage metal hydride system as topping cycle in cascading sorption systems for cold generation. Applied Thermal Engineering 2002;22:631–9.
[120] Qin F, Chen J, Lu M, Chen Z, Zhou Y, Yank K. Development of a metal hydride refrigeration system as an exhaust gas-driven automobile air conditioner. Renewable Energy 2007;32:2034–52.
[121] Ni J, Liu H. Experimental research on refrigeration characteristics of a metal hydride heat pump in auto air-conditioning. International Journal of Hydrogen Energy 2007;32:2567–72.
[122] Linder M, Mertz R, Laurien E. Experimental results of a compact thermally driven cooling system based on metal hydrides. International Journal of Hydrogen Energy 2010;35:7623–32.
[123] Dehouche Z, de Jong W, Willers E, Isselhorst A, Groll M. Modelling and Simulation of Heating/Air Conditioning Systems using the Multi-Hydride-Thermal-Wave concept. Applied Thermal Engineering 1998;18(6):457–80.
[124] Willers E, Groll M. Evaluation of metal hydride machines for heat pumping and cooling applications. International Journal of Refrigeration 1999;22: 47–58.
[125] Kato Y. Chemical energy conversion technologies for efficient energy use. Thermal Energy Storage for Sustainable Energy Consumption. Netherlands: Springer; 2007 pp 377-391.
[126] Kato Y, Yamashita N, Kobayashi K, Yoshizawa Y. Kinetic study of the hydration of magnesium oxide for a chemical heat pump. Applied Thermal Engineering 1996;16:853–62.
[127] Kato Y. Packed bed reactor demonstration of magnesium oxide/water chemical heat pump. In: Proceedings of the 11th International Conference on Thermal Energy Storage—Effstock 2009 Stockholm, Sweden; 2009.
[128] Kato Y, Kobayashi K, Yoshizawa Y. Durability to repetitive reaction of magnesium oxide/water reaction system for a heat pump. Applied Thermal Engineering 1998;18:85–92.
[129] Kato Y, Nakahata J, Yoshizawa Y. Durability characteristics of the hydration of magnesium oxide under repetitive reaction. Journal of Material Sciences 1999;34:475–80.
[130] Kato Y, Saito T, Soga T, Ryu J, Yoshizawa Y. Durable reaction material development for magnesium oxide/water chemical heat pump. Journal of Chemical Engineering of Japan 2007;40:1264–9.
[131] Kato Y, Sasaki Y, Yoshizawa Y. Magnesium oxide/water Chemicals heat pump to enhance energy utilization of a cogeneration system. Energy 2005;30:2144–55.
[132] Kato Y, Takahashi R, Sekiguchi T, Ryu J. Study on medium-temperature chemical heat storage using mixed hydroxides. International Journal of Refrigeration 2009;32:661–6.
[133] Ryu J, Takahashi R, Hirao N, Kato Y. Effect of metal mixing on reactivities of magnesium oxide for chemical heat pump. Journal of Chemical Engineering of Japan 2003;40:1281–6.
[134] Kim ST, Ryu J, Kato Y. Reactivity enhancement of chemical materials used in packed bed reactor of chemical heat pump. Progress in Nuclear Energy 2011;53(7):1027–33.
[135] Ogura H, Mujumdar AS. Proposal for a novel chemical heat pump dryer. Drying Technology 2000;18(4-5):1033–53.
[136] Ogura H, Yamamoto T, Otsubo Y, Ishida H, Kage H, Mujumdar AS. Controllability of a Chemicals heat pump dryer. In: Proc Drying 2004—14th International Drying Symposium São Paulo, Brazil; 2004. pp 998–1004.
[137] Ogura H, Ishida H, Yokooji R, Kage H, Matsuno Y, Mujumdar AS. Experimental studies on a novel chemical heat pump dryer using a solid–gas reaction. Drying Technology 2001;19(7):1461–77.
[138] Ogura H, Yasuda S, Otsubo Y, Mujumdar AS. Continuous operation of a chemicals heat pump. Asia-Pacific Journal of Chemical Engineering 2007;2: 118–23.
[139] Cerkvenik B, Storkenmaier F, Kato Y. Use of CaO/H2O reversible reaction for cooling. In: Proceedings of the 2nd Workshop and Expert meeting, Annex 17 Ljubljana, Slovenia; 2002.
[140] Cerkvenik B, Satzger P, Ziegler F, Poredos A. High Efficient Cycles using CaO/H_2O and $LiBr/H_2O$ for Gas Cooling. In: Proceedings of the 6th ASME Conference on Renewable and Advanced Energy Systems for the 21th century Maui, Hawaii; 1999.
[141] Depta G. Messaparatur fuer gas-feststoff-reaktionen in waermepumpen. Munich: Technische Universität München; 1994.
[142] Kato Y, Saku D, Harada N, Yoshizawa Y. Utilization of high temperature heat from nuclear reactor using inorganic chemicals heat pump. Progress in Nuclear Energy 1998;32:563–70.
[143] Kato Y, Harada N, Yoshizawa Y. Kinetic feasibility of a Chemicals heat pump for heat utilization of high-temperature processes. Applied Thermal Engineering 1999;19:239–54.
[144] Kato Y, O-shima T, Yoshizawa Y. Thermal performance of a packed bed reactor for a high-temperature. Chemicals heat pump. International Journal of Energy Research 2001;25:577–89.
[145] Kato Y, Yamada M, Kanie T, Yoshizawa Y. Calcium oxide/carbon dioxide reactivity in a packed bed reactor of a Chemicals heat pump for high-temperature gas reactors. Nuclear Engineering and Design 2011;210(1-3):1–8.